

# CAUSAL CLASSIFICATION OF PATHOLOGICAL MISNER-TYPE SPACETIMES

N. E. RIEGER

MATHEMATICS DEPARTMENT, UNIVERSITY OF CALIFORNIA IRVINE, ROWLAND HALL, 92697 IRVINE, USA

CURRENT ADDRESS: MATHEMATICS DEPARTMENT, YALE UNIVERSITY, 219 PROSPECT STREET, NEW

HAVEN, CT 06520, USA

N.RIEGER@YALE.EDU

**ABSTRACT.** We analyze the Misner space, incorporating Kip Thorne’s ‘moving wall’ model, and pseudo-Schwarzschild spacetime, exploring their geometric structures, geodesics, and causal properties. We propose that pseudo-Schwarzschild spacetime serves as a non-flat generalization of Misner space. We then introduce the pseudo-Reissner-Nordström spacetime, a novel chronology-violating model that extends the previous two frameworks and unifies the geodesic structures of all three spacetimes. We suggest that these spacetimes constitute a causality-violating family, interconnected through common fundamental causal features—geodesics, Cauchy and chronology horizons, and acausal regions—leading to a conjecture that they are isocausal.

**This article is based on research originally conducted as part of a project during 2016-2018 under the supervision of Kip S. Thorne.**

## 1. INTRODUCTION

General relativity defines a class of cosmological models, each representing an idealization of a physically possible universe compatible with the theory. A cosmological model is a mathematical description of this idealized universe, referred to as a spacetime and represented by a pair  $(M, g)$ . Here,  $M$  is a differentiable manifold that captures the topology and continuity of the universe, while  $g$  is a smooth, symmetric, non-degenerate  $(0, 2)$ -tensor field on  $M$ . The metric tensor  $g$  encodes the geometric and causal structure of spacetime, with each point in  $M$  representing a possible event. In this context, the theoretical possibility of time travel—through closed timelike curves that allow a timelike observer to return to an event in his own past—has been studied extensively within general relativity [1, 4, 9, 19, 12, 21, 22]. In 1967 Charles Misner introduced the Misner space [14] as a basic spacetime with a chronology violating region. However, while it is relatively simple to construct spacetimes containing closed timelike curves, finding examples that are also realistic, to some extent, is more challenging. The more sophisticated causality violating pseudo-Schwarzschild spacetime, proposed by Amos Ori [16] in 2007, offers a more realistic alternative to idealized black hole models by incorporating internal features such as Cauchy horizons, avoiding singularities, and reflecting the breakdown of determinism inside black holes.<sup>1</sup>

We begin by examining those two seemingly different spacetimes, the Misner space, also incorporating Kip Thorne’s ‘moving wall’ model, and pseudo-Schwarzschild spacetime. We aim to shed light on their

---

<sup>1</sup>An "idealized black hole model" is a simplified theoretical depiction of a black hole, commonly assuming perfect spherical symmetry and no rotation, and typically derived from the Schwarzschild metric.

geometric structures and causal properties, with a particular focus on pathologies. These two spacetimes are related through their chronological and global properties. Our findings suggest that the pseudo-Schwarzschild spacetime can be viewed as a non-flat generalization of Misner space. By examining the relationship between the pseudo-Schwarzschild and Misner spacetimes, we put forward a conjecture in 2016 that these spacetimes are isocausal [18].

We introduce a novel chronology-violating spacetime, referred to as the pseudo-Reissner-Nordström spacetime. This model represents a further generalization of the previous two spacetime frameworks. We derive the pseudo-Reissner-Nordström spacetime from the well-known Reissner-Nordström spacetime and review our main results within this more general framework. By situating our findings within this broader context, we conclude that these spacetimes—all of which share a similar geodesic structure, along with Cauchy and chronology horizons, and acausal regions—form a causality-violating family.

Ultimately, all of these spacetimes can be expressed in a warped product form, with their metrics decomposing into cylindrical and hyperbolic components. From a purely mathematical standpoint, the resulting similarities in causal properties might seem unsurprising. However, from a physics perspective, these interrelationships are noteworthy. The spacetimes in question differ significantly in their physical interpretation and geometric origin—ranging from a flat vacuum solution of the Einstein equations, to an asymptotically flat black hole solution of the vacuum field equations, to a spacetime that violates the weak energy condition and requires so-called ‘exotic matter’ as its source. Despite these differences, all exhibit analogous causal behavior. This distinction is crucial, as it sets the pseudo-Reissner-Nordström spacetime apart from both the Misner and pseudo-Schwarzschild spacetimes, which are vacuum solutions. The non-vacuum nature of the pseudo-Reissner-Nordström spacetime is precisely what makes its inclusion in the family of causality-violating spacetimes both surprising and significant.

The intricate interrelationships of those spacetimes offer a unified framework for understanding their causal and geometric features, motivating the conjecture that all three spacetimes are isocausal. While the conjecture is supported by our preliminary analysis and the foundational basis outlined in this article, the formal proof will be presented in future work.

**1.1. Causality violating spacetimes.** Before presenting the main results we want to review some useful definitions.

First, recall that a Lorentzian manifold  $M$  is said to be *past-distinguishing* if any two points  $p, q \in M$  with identical chronological pasts must coincide; that is,  $I^-(p) = I^-(q) \implies p = q$ . Similarly,  $M$  is said to be *future-distinguishing* if any two points  $p, q \in M$  the same chronological future must be identical:  $I^+(p) = I^+(q) \implies p = q$ . We say a spacetime satisfies the *distinguishability condition* if it is both, past- and future-distinguishing. Thus, a Lorentzian manifold is *not* past-distinguishing if distinct points can have identical pasts. A spacetime allows time travel if a point  $p \in M$  lies in its own timelike future, i.e.,  $p \in I^+(p)$ , resulting in a closed timelike curve that violates causality. Hence, for distinct points  $p, q \in M$ , it is possible to have  $p \ll q \ll p$ . The *chronology violating region* of a spacetime  $(M, g)$  is defined as  $\mathcal{V}(M) = \{p \in M : p \in I^+(p)\}$ .<sup>2</sup>

---

<sup>2</sup>The set  $\mathcal{V}(M)$  decomposes into equivalence classes  $[p]$ , where  $p \sim q$  if  $p \ll q \ll p$ . That is, two points  $p, q \in [p]$  belong to the same equivalence class if there exists a closed timelike curve  $\gamma$  connecting  $p$  and  $q$  with  $\gamma(I) \subset [p]$ . Points within the same equivalence class share the same chronological character, making it impossible to establish a definite chronological order of events among them.

**Definition 1.1.** A spacetime  $(M, g)$  is said to be *chronological* and to satisfy the *chronology condition* if it does not contain any closed timelike curves; that is,  $p \notin I^+(p)$  for all  $p \in M$ .

**Proposition 1.2.** [10] *If the spacetime  $(M, g)$  is compact then the chronology violating region is not empty and contains a closed timelike curve.*

**Definition 1.3.** A subset  $S \subset M$  is said to be *achronal* if no timelike curve intersects it more than once; that is, there do not exist points  $p, q \in S$  such that  $q \in I^+(p)$ . Equivalently,  $I^+(S) \cap S = \emptyset$ .

The boundaries separating chronal and achronal regions are called *chronology horizons*. The chronal region ends and closed timelike curves arise at the future chronology horizon. Conversely, closed timelike curves vanish and the chronal region begins at the past chronology horizon. A future chronology horizon is a special type of future Cauchy horizon and it is therefore subject to all the properties of such horizons [5]. The *past chronology horizon* is defined dually.

**Definition 1.4.** Let  $J^-(U)$  denote the causal past of a set  $U \subset M$ , and let  $\bar{J}^-(U)$  represent the topological closure of  $J^-$ . Define  $\mathcal{I}^+$  and  $\mathcal{I}^-$  as future and past null infinity, respectively. The *boundary* of  $\bar{J}^-$  is given by  $\partial\bar{J}^-(U) = \bar{J}^-(U) \setminus J^-(U)$ , and the *future event horizon* of  $M$  is  $\mathcal{H}^+ = \partial\bar{J}^-(\mathcal{I}^+)$ .

The event horizon is often referred to as the ‘‘point of no return’’. It is useful to define  $\bar{J}^-(\mathcal{I}^+)$  as the *domain of outer communications*. The complement  $M \setminus \bar{J}^-(\mathcal{I}^+)$  is then referred to as the *black hole* (region). A spacetime may contain a singularity in several senses. In this context, a singularity is a hypersurface on which all worldlines that pass through the event horizon terminate.

## 2. MISNER SPACE

Misner space [14], typically presented as a 2-dimensional toy model, is a type of spacetime in general relativity that illustrates how singularities might form. This spacetime begins with causally well-behaved initial conditions but later develops closed timelike curves, leading to a chronology-violating region. Characterized by a conformally flat metric, Misner space is also Ricci-flat, making it a valid vacuum solution to Einstein’s field equations in the absence of matter and energy. The 4-dimensional version can be obtained as a straightforward extension. It can be considered as Minkowski space with an altered topology due to identification under a boost.<sup>3</sup> To see this, start with the Lorentz-Minkowski spacetime  $\mathcal{M} := (\mathbb{R}^4, \tilde{\eta})$ , defined as the smooth manifold  $\mathbb{R}^{1,3} := (\mathbb{R}^4, \tilde{\eta})$  equipped with Lorentzian coordinates  $(\tilde{t}, \tilde{x}_1, \tilde{x}_2, \tilde{x}_3)$ . These coordinates yield the metric tensor  $\tilde{\eta}$ , given by

$$(2.1) \quad ds^2 := -d\tilde{t}^2 + (d\tilde{x}_1)^2 + (d\tilde{x}_2)^2 + (d\tilde{x}_3)^2.$$

This coordinate system for Minkowski spacetime is related to Misner coordinates  $(\eta, X_1, X_2, X_3)$  through the following coordinate transformation

$$(2.2) \quad \tilde{t} = 2\sqrt{-\eta} \cosh\left(\frac{X_1}{2}\right), \quad \tilde{x}_1 = 2\sqrt{-\eta} \sinh\left(\frac{X_1}{2}\right), \quad \tilde{x}_2 = X_2, \quad \tilde{x}_3 = X_3.$$

This coordinate change results in the Misner metric  $ds^2 = -\eta^{-1}d\eta^2 + \eta(dX_1)^2 + (dX_2)^2 + (dX_3)^2$ , where  $0 < \eta < \infty$ ,  $0 \leq X_1 \leq 2\pi$ , and  $0 \leq X_2, X_3 \leq \infty$ . Due to the periodic nature of the coordinate  $X_1$ , the Misner spacetime is defined on  $S^1 \times \mathbb{R}^3$ . Accordingly, Minkowski space  $\mathcal{M}$  serves as the associated covering space of Misner space, where identical points are determined by the identification

<sup>3</sup>A Lorentz boost is a Lorentz transformation with no rotation.

$$(2.3) \quad (\tilde{t}, \tilde{x}_1, \tilde{x}_2, \tilde{x}_3) \leftrightarrow (\tilde{t} \cosh(na) + \tilde{x}_1 \sinh(na), \tilde{t} \sinh(na) + \tilde{x}_1 \cosh(na), \tilde{x}_2, \tilde{x}_3),$$

with  $a$  is the period associated with the periodic direction  $X_1$ .<sup>4</sup> However, at  $\eta = 0$  the metric exhibits an apparent (coordinate) singularity. To address this, we introduce a new set of coordinates to extend the metric beyond  $\eta = 0$ . Define  $\varphi = X_1 - \ln(\eta)$ , which transforms the metric into

$$(2.4) \quad ds^2 = 2dTd\varphi + Td\varphi^2 + (dX_2)^2 + (dX_3)^2,$$

where  $T$  is a time-like coordinate and  $\varphi$  is an angular coordinate, with domains  $-\infty < T < \infty$  and  $0 \leq \varphi \leq a$ .<sup>5</sup>

Note that this is only one of two possible inequivalent extensions of Misner space. Alternatively, we could start with the Minkowski metric (2.1) again, but apply a different coordinate transformation, subsequently extending the resulting Misner space across the coordinate singularity in a different way. In both cases, we obtain a cylindrical Misner spacetime defined on  $M = S^1 \times \mathbb{R}^3$ .

We time orient the Misner space by requiring  $-\partial_T$  to be future-pointing. It is evident that  $\partial_T$  is always lightlike, while  $\partial_\varphi$  is spacelike for  $T > 0$ , lightlike for  $T = 0$ , and timelike for  $T < 0$ , respectively. At  $T = 0$ , there is a null surface, called the *chronology horizon*, which separates the region of chronology violation from the chroral region. Every causal curve intersects this surface exactly once, making it the Cauchy horizon for any initial hypersurface with  $T_0 = \text{const} > 0$ . Any hypersurface where  $T = \text{const} > 0$  is spacelike and can be chosen as an initial hypersurface for specifying initial data.

**Proposition 2.1.** *If a closed timelike curve (CTC) arises in a chronology-violating spacetime, then it contains an unlimited number of CTCs.*

*Proof.* Let  $\alpha$  be a closed timelike curve in the spacetime  $M$ . Then consider two points  $p$  and  $q$  on  $\alpha$  that satisfy the condition  $p \ll q$ . Consequently, we have  $p \ll q \ll p$  and  $p \in I^+(p)$  as well as  $q \in I^+(q)$ . The same applies for the timelike past. The sets  $I^+(p)$  and  $I^-(q)$  are open and their finite intersection  $O := I^+(p) \cap I^-(q)$  is therefore not empty and an open set as well. Choose now any  $r \in O$ . Since  $r \in I^+(p)$  there is a future directed timelike curve segment from  $p$  to  $r$ , and because  $r \in I^-(q)$ , there is a future directed timelike curve segment from  $q$  to  $r$ . It remains to join the two curve segments at the point  $r$  which can be done smoothly due to the fact that  $O$  is an open neighborhood of  $r$ .  $\square$

The location at which closed timelike curves first emerge is called the *chronology horizon*. It separates a chroral region (without CTCs) from a non-chroral region that contains CTCs at every point. It is a well known fact that Misner space contains closed timelike curves, but above all it follows from Section 2.2 below, Misner space also comprises closed timelike geodesics.

**2.1. Kip Thorne's physics approach to Misner space.** Kip Thorne's interpretation of Misner space, inspired by extensive discussions with Charles Misner, offers a distinct and highly engaging perspective, as also presented in [22]. This subsection builds on Thorne's insights to further explore the nature of Misner space.

<sup>4</sup>Note, that these points correspond to  $(\eta, X_1, X_2, X_3) \leftrightarrow (\eta, X_1 + na, X_2, X_3)$  in Misner coordinates.

<sup>5</sup>Due to the periodicity condition,  $\varphi$  can take any real number value. Specifically,  $\varphi$  and  $\varphi + na$  are equivalent for any integer  $n$ .

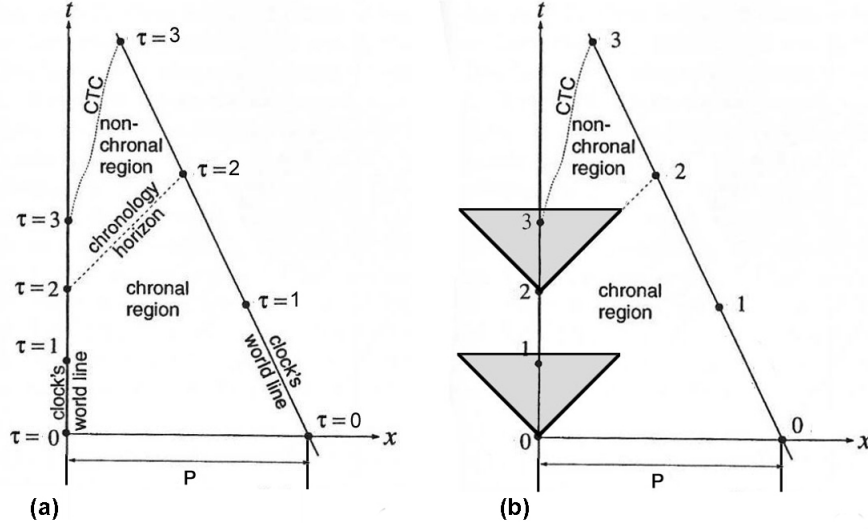


FIGURE 1. Depicted are two spacetime diagrams for Misner space, illustrating the occurrence of closed timelike curves (CTCs). The symbol  $\tau$  denotes proper time, and it is important to note that identical values of proper time on both axes are physically identical. CTCs appear due to the time dilation effects of special relativity. The light cone structure is shown in Figure (b). Through every event to the future of the chronology horizon, there exist CTCs, whereas there are no CTCs to the past of the chronology horizon.

Consider the flat 2-dimensional Minkowski spacetime with a reference frame in Lorentzian coordinates  $(t, x)$ , where  $t$  is interpreted as the time direction and  $x$  as the space direction. Next, we identify the  $t$ -axis at  $x = 0$  with the  $t$ -axis at  $x = P$  (which we will henceforth refer to as the  $\bar{t}$ -axis):  $(t, P) \sim (t, 0)$ . At  $t = 0$ , we set the  $\bar{t}$ -axis into motion with constant speed  $\beta$  towards the  $t$ -axis, while the reference frame in Lorentzian coordinates remains at rest with respect to the  $t$ -axis. We can think of the  $t$ -axis as representing an observer at rest and the  $\bar{t}$ -axis as representing an observer moving at speed  $-\beta$  relative the reference frame. This moving observer is equipped with a clock, and  $\tau$  denotes the proper time measured by this clock.<sup>6</sup> This  $x, t$ -coordinate system is furnished with the flat Minkowski metric  $\tilde{\eta}$ , and therefore the light cones do not tilt or open. Due to the special relativistic time dilation, a region with closed timelike curves develops, see Figure 1.

Note that the worldline of the clock at rest (along the  $t$ -axis) and the worldline of the clock in motion (along the  $\bar{t}$ -axis) are identified by  $\sim$ , meaning the events along these lines are physically identical. However, due to special relativity, the observer at rest perceives the moving clock to tick more slowly. On the  $t$ -axis we have  $\tau = t$ , while on the  $\bar{t}$ -axis, due to time dilation,  $\tau = \frac{t}{\sqrt{1-\beta^2}} = \gamma t$ , where  $\gamma := \frac{1}{\sqrt{1-\frac{v^2}{c^2}}} = \frac{1}{\sqrt{1-\beta^2}}$ .

<sup>6</sup>Proper time, also called clock time or process time, is a measure of the amount of physical process that a system undergoes.

**Connection to mathematical approach.** In the style of [12], we set the proper time origins,  $\tau = 0$ , such that they are separated by the chronology horizon at  $x = t$ . We denote the spatial distance between these  $\tau = 0$  origins as  $D$ .

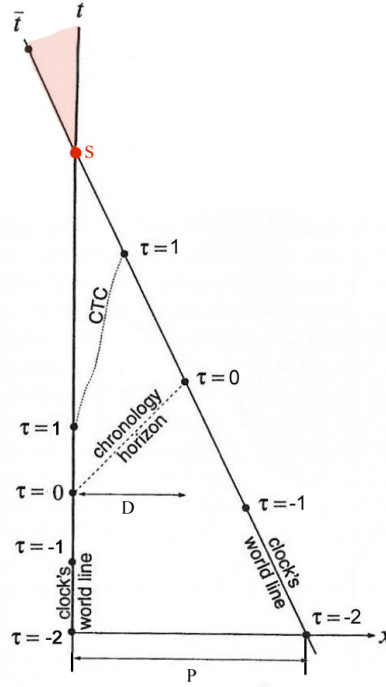


FIGURE 2. ‘Moving wall’ Misner space with proper time origins, such that the two walls are separated by the chronology horizon at  $x = t$  by the spatial distance  $D$ .

The left wall ( $t = \tau$ ,  $x = 0$ ) in this example is at rest in Lorentzian coordinates, while the right wall ( $x = D - \beta\gamma\tau$ ,  $t = D + \gamma\tau$ ) moves towards the left one with constant velocity  $\beta$ . The location of the chronology horizon depends on  $D$ , which can be any positive constant, and the speed  $\beta$  with  $|\beta| < 1$ . All further boosted copies of Misner space depend on this initial choice of  $D$  and  $\beta$ . Provided  $\beta \neq 0$ , the two walls intersect at a the point  $s$ , see Figure 2. This point, as well as the region beyond it, raises questions about their nature. We can better address these questions with the aid of the covering space, as depicted in Figure 3.

**Calculation of intersection points.** We can describe the ‘moving wall’ model of Misner space by switching to the covering space [22]. Side by side, we line up copies of Misner space that are identified through the action of a boost with speed  $\beta$ . In comparison to Figure 2,  $W_0$  corresponds to  $t$ , and  $W_1$  corresponds to  $\bar{t}$ . Additionally, the boost induces an equivalence relation, identifying boost-related points  $p$  under  $\sim$ , all of which lie on hyperbolas defined by  $\bar{t}^2 - \bar{x}^2 = \text{const}$ .

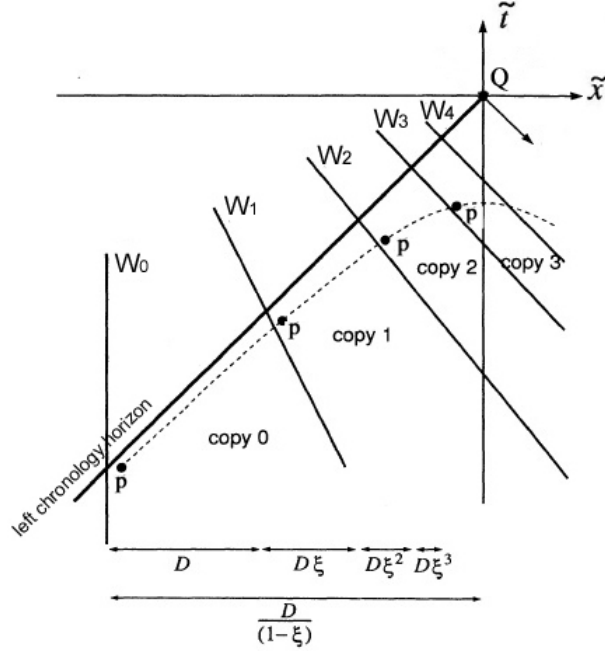


FIGURE 3. Covering space for the ‘moving wall’ model of Misner space. The singularity manifests as the intersection point  $Q$  of the left and right chronology horizons.

The relation between the covering space in Minkowski coordinates  $(\tilde{t}, \tilde{x})$  and the Minkowski coordinates  $(t, x)$  in the ‘moving wall’ model of Misner space (*copy 0*) is given by [12]

$$(2.5) \quad \tilde{t} = t - \frac{D}{1-\xi}$$

and

$$(2.6) \quad \tilde{x} = x - \frac{D}{1-\xi},$$

where  $\xi = \sqrt{\frac{1-\beta}{1+\beta}}$  is the Doppler blueshift. In the covering space (Figure 3) we get the spatial distance between  $W_0$  and the  $\tilde{t}$ -axis by the converging series

$$D\xi^0 + D\xi^1 + D\xi^2 + D\xi^3 \dots = D \cdot \sum \xi^i = D \cdot \frac{1}{1-\xi},$$

for  $|\xi| < 1$ . Thus, the left wall of *copy 0*, denoted  $W_0$ , is located at  $\tilde{x} = \frac{-D}{1-\xi}$ , and the right wall,  $W_1$ , of *copy 0* is located at

$$(\tilde{t} + \frac{\xi D}{1-\xi}) = (\frac{1+\xi^{-2}}{1-\xi^{-2}})(\tilde{x} + \frac{\xi D}{1-\xi}).$$

Hence,

$$(2.7) \quad (\frac{1+\xi^{-2(n+1)}}{1-\xi^{-2(n+1)}})(\tilde{x} + \frac{\xi^{n+1}D}{1-\xi}) - \frac{\xi^{n+1}D}{1-\xi} = (\frac{1+\xi^{-2n}}{1-\xi^{-2n}})(\tilde{x} + \frac{\xi^n D}{1-\xi}) - \frac{\xi^n D}{1-\xi}$$

yields the intersection of two adjacent walls,  $W_n \cap W_{n+1} = s_n = (\tilde{t}_n, \tilde{x}_n)$ :

$$(2.8) \quad \tilde{t}_n = \frac{D\xi^{-n}(\xi^{1+2n} - 1)}{\xi^2 - 1}$$

$$(2.9) \quad \tilde{x}_n = \frac{D\xi^{-n}(\xi^{2n+1} + 1)}{\xi^2 - 1}.$$

Each point  $s_n$  is on the hyperboloid

$$(2.10) \quad \tilde{t}_n^2 - \tilde{x}_n^2 = -\frac{4\xi D^2}{(\xi^2 - 1)^2} = \text{const.}$$

Clearly, we have  $\tilde{t}_{n+1}^2 - \tilde{x}_{n+1}^2 = \tilde{t}_n^2 - \tilde{x}_n^2$  so the points  $s_{n+1}$  and  $s_n$  lie on the same hyperboloid. From this, we can conclude that each point  $s_n$  is taken by a boost to  $s_{n+1}$ . Thus, the points  $s_n$  belong to the same fiber over a specific point in the Misner base space and can be regarded as physically identical, as they are mapped by the covering map onto identical events in Misner space.

We turn again to the covering space (see Figure 4), we focus on the intersection points and the regions beyond them. At first glance, the seemingly inconsistent distribution of intersection points  $s_n$  might appear to contradict the definition of the covering space, which is constructed as a union of disjoint sets (in our case, a disjoint union of copies of Misner space). However, this non-chronological structure simply reflects the chronology-violating nature of region *III*, as explained in [11].

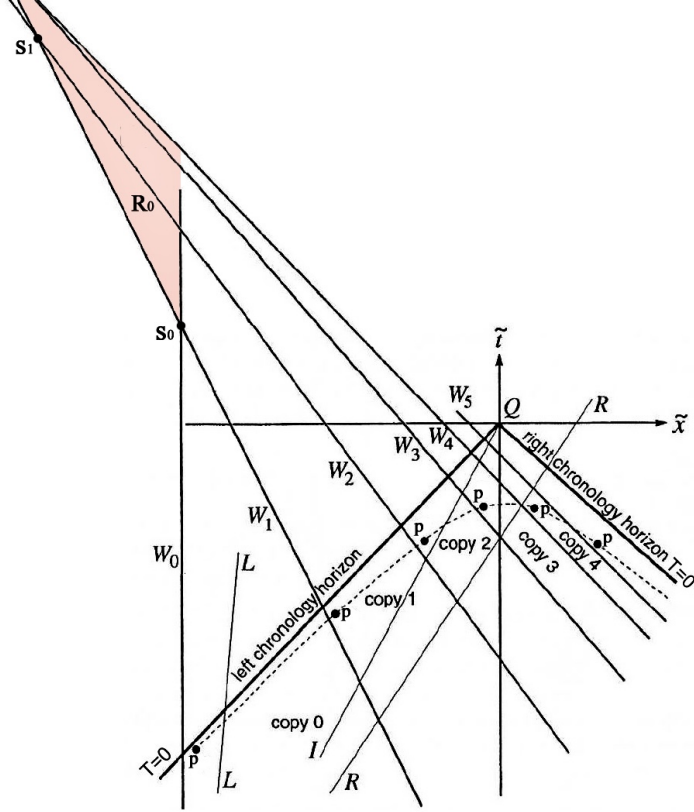


FIGURE 4. The covering space for ‘moving wall’ model of Misner space illustrates the intersection points  $s_n$  and the corresponding regions  $R_n$  which are mirror-inverted to the respective region below  $s_n$ .

The above considerations, along with the fact that our initial choice of  $D$  was arbitrary, lead to the conclusion that the intersection points depend specifically on the choice of the parameter  $D$ . Consequently, we may denote these intersection events as  $s_n(D)$ . If the parameter  $D$  is changed,  $s_n(D)$  moves along the parabola given by (see Equation (2.10))

$$f(D) = -\frac{4\xi}{(\xi^2 - 1)^2} \cdot D^2.$$

To summarize, this ensures that the intersection points  $s_n$  are not physical singularities, but merely coordinate singularities. This reasoning is supported by the fact that the 2-dimensional Misner universe can be viewed as a simplified  $2D$  wormhole spacetime [12]; both spacetimes share the same covering space. By projecting a wormhole whose mouths move past each other at speed  $\beta$  [21, Figure 3c] onto the  $x - t$  plane, we obtain a situation similar to that of Misner space, as described above. However, this wormhole spacetime diagram reveals a new feature: a past chronology horizon,  $\mathcal{H}_-$ . Therefore, the chronology-violating region is confined

by two chronology horizons. Like the future chronology horizon  $\mathcal{H}_+$ , the past chronology horizon  $\mathcal{H}_-$  is a null surface.

Given that the initial choice of the wall  $W_0$  and the speed  $\beta$  are arbitrary, we can obtain the covering space without coordinate singularities [17] by appropriately selecting these initial conditions (as shown in Figure 5). The covering space corresponds to the left half-plane of Minkowski space.

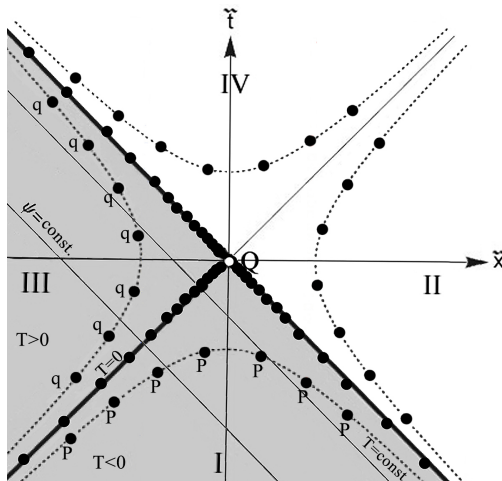


FIGURE 5. Universal covering space for Misner space with the metric  $ds^2 = Td\psi^2 + 2dTd\psi$ . The transformation between the covering space coordinates and Misner coordinates is given by  $\psi = -2\ln(\frac{\tilde{t}-\tilde{x}}{2})$ ,  $T = \frac{\tilde{t}^2-\tilde{x}^2}{4}$ .

**2.2. Geodesics for warped Misner product space.** The 4-dimensional Misner space (2.4) can be expressed as a warped product space of the form  $M = M_Z \times_r H^2$ , where  $M_Z$  is the 2-dimensional Misner-type spacetime with coordinates  $(T, \varphi)$ , and  $H^2$  is the 2-dimensional hyperbolic plane, described by coordinates  $(\theta, \phi)$ . The general form of the metric combines the 2-dimensional Misner-type geometry, which encodes the non-trivial topological and causal structure, with a 2-hyperbolic plane that introduces hyperbolic symmetry. The metric can be written as

$$ds^2 = f(T)(d\varphi)^2 + 2dTd\varphi + r^2(d\theta^2 + \sinh^2 \theta d\phi^2),$$

where  $f(T)$  describes the time-dependent geometry of the Misner-type spacetime and  $r$  is the warping function. To interpret this, we consider  $\mathbb{R}^2$  as being represented topologically by the hyperbolic plane  $H^2$ . The 4-dimensional Misner space can then be described as a warped product  $M := M_Z \times_r H^2$ , with the warping function  $r$  being a scalar function  $r : M_Z \rightarrow \mathbb{R}$ , depending on the coordinates of the base manifold  $M_Z$ . The Misner space  $M_Z = S^1 \times \mathbb{R}$  is equipped with the cylindrical metric  $ds^2 = 2dTd\varphi + Td\varphi^2$ . The fiber  $H^2$ , with coordinates  $(\theta, \phi)$ , has the hyperbolic metric  $g_{H^2} = d\theta^2 + \sinh^2 \theta d\phi^2$ , scaled by  $r^2$ . Therefore, the metric on the total space  $M$  can be written as  $ds^2 = g_Z + r^2 g_{H^2}$ , which explicitly expands to

$$ds^2 = 2dTd\varphi + Td\varphi^2 + r^2(d\theta^2 + \sinh^2 \theta d\phi^2),$$

where the warping function  $r$  is given by  $r = T \exp(\frac{\varphi}{2}) - \exp(-\frac{\varphi}{2})$ . If  $r$  is constant, the warped product reduces to a direct product of the base  $M_Z$  and fiber  $H^2$ .

*Remark 2.2.* The surface  $H_r^2$ , also known as a pseudo-sphere, has constant negative Gaussian curvature of  $-1$ , which provides the desired high symmetry. The upper sheet of the pseudo-sphere is given by the set

$$H_r^2 = \{(z, x, y) \in \mathbb{R}_1^3 : -z^2 + x^2 + y^2 = -r^2, z > 0\}.$$

Based on the warped geometry of Misner space, we can focus on the embedded cylinders defined by  $\theta = \text{const}$  and  $\varphi = \text{const}$ . By doing so, we restrict our attention to the 2-dimensional Misner cylinder  $M_Z$ , which captures the essential features of the Misner-type geometry.

Here, we examine the geodesic equations, which show that there exist incomplete null and timelike geodesics that spiral around the cylinder and cannot be extended. One class of these incomplete timelike geodesics not only orbits around the chronology horizon but also penetrates the null surface into negative  $T$ , where it reaches a turning point, intersects itself, and then encircles the cylinder below the horizon.

Given the 2-dimensional Misner metric  $ds^2 = Td\varphi^2 + 2dTd\varphi$ , null geodesics are described by

$$(2.11) \quad \begin{cases} \psi(T) = \text{const.} & (\text{outgoing}) \\ \psi(T) = \int -\frac{2}{T}dT & (\text{ingoing}) \end{cases},$$

where outgoing null geodesics are complete, while ingoing ones circle around the Misner cylinder infinitely often near the Cauchy horizon. For timelike geodesics, we use the expression

$$(2.12) \quad \psi(T) = \int \frac{\dot{\psi}}{\dot{T}} dT.$$

Substituting  $\dot{\psi}$  and  $\dot{T}$ , we get:

$$\psi(T) = \frac{\frac{1}{T}(\xi - \omega\sqrt{\xi^2 + T})}{\omega\sqrt{\xi^2 + T}} dT = \int \frac{1}{T} \left( \frac{\omega}{\sqrt{1 + \frac{T}{\xi^2}}} - 1 \right) dT,$$

with  $\xi \equiv \text{const}$  and  $\omega = \pm 1$  for outgoing and ingoing geodesics, respectively. There are two families of timelike geodesics and both of them are incomplete. One class of geodesics does not cross the Cauchy horizon and spirals around the cylinder just above  $T = 0$ . A geodesic from the other class, however, crosses the Cauchy horizon, entering the chronology-violating region. It reaches a turning point at  $T = -\xi^2$ , where the particle's velocity vanishes, as shown by the condition

$$\omega\sqrt{\xi^2 + T} = 0 \Leftrightarrow \sqrt{\xi^2 + T} = 0 \Leftrightarrow T = -\xi^2.$$

Therefore, a massive particle cannot reach  $T = -\infty$ . Such a timelike geodesic intersects itself as it tracks back, converging towards the Cauchy horizon and spiraling around the Misner cylinder just below  $T = 0$ . In contrast, there is no such behavior for photons, and there is no obstruction for null geodesics to reach  $T = -\infty$ .

This result implies that geodesics encircle the extended Misner cylinder with increasingly higher frequencies as they approach  $T = 0$ , asymptotically nearing the chronology horizon. The singular point  $Q$  represents

a genuine spacetime pathology: geodesic incompleteness in this case could correspond to a rocket ship suddenly disappearing from the universe after a finite amount of proper time. As shown in Subsection 2.1, this pathological nature of the geodesics becomes evident in the covering space, where the geodesic singularity manifests as the intersection point  $Q$  of the left and right chronology horizons [22], as illustrated in Figure 4.

### 3. GENERAL EQUATIONS FOR RADIAL GEODESICS

In this section, we present a complete canonical formulation of the geodesic equations for cylindrical Misner-type spacetime models, focusing on the embedded  $\theta = \text{const}$  and  $\varphi = \text{const}$  cylinders, as introduced in Subsection 2.2. We anticipate that the radial geodesic equations for the pseudo-Schwarzschild and pseudo-Reissner-Nordström spacetimes (to be discussed in Sections 4 and 6) will exhibit structural similarities. To unify these cases, we derive a general form of the geodesic equations, which proves to be valid for all three hyperbolically symmetric spacetimes. Notably, this general form can also be applied to Misner space, recognizing that the 2-dimensional Misner metric,  $ds^2 = Td\varphi^2 + 2dTd\varphi$ , can be rewritten in the canonical form

$$(3.1) \quad ds^2 = f(r)d\nu^2 + 2d\nu dr,$$

where  $f(r) = g_{\nu\nu}$ . This metric, due to its geodesic singularity at  $Q$ , is commonly referred to as the canonical quasi-singular metric [13].

To generalize the Equation 3.1 to the 4-dimensional case for hyperbolically symmetric models, we start with the general form of a hyperbolically symmetric metric given by

$$(3.2) \quad ds^2 = g_{\nu\nu}d\nu^2 + 2g_{\nu r}d\nu dr + r^2(d\theta^2 + \sinh^2\theta d\phi^2).$$

Since we are strictly interested in geodesics for radial motion, we can safely set  $\phi = 0$  and  $\theta = \frac{\pi}{2}$ . Furthermore, we impose the metric condition resulting from the causal character of the geodesics

$$(3.3) \quad g_{\nu\nu}\dot{\nu}^2 + 2g_{\nu r}\dot{\nu}\dot{r} \equiv k,$$

where  $k = -1$  for timelike,  $k = +1$  for spacelike, and  $k = 0$  for null geodesics. The time coordinate  $\nu$  is cyclic, and we always have  $g_{\nu r} = 1$ , so we obtain the constant term

$$\frac{\partial(\frac{1}{2}g_{\nu\nu}\dot{\nu}^2 + \dot{\nu}\dot{r})}{\partial\dot{\nu}} = g_{\nu\nu}\dot{\nu} + \dot{r} \equiv \xi.$$

This is equivalent to  $\dot{\nu} = g^{\nu\nu}(\xi - \dot{r})$ , and substituting this into Equation (3.3) gives

$$g_{\nu\nu}[g^{\nu\nu}(\xi - \dot{r})]^2 + 2\dot{r}[g^{\nu\nu}(\xi - \dot{r})] = k \iff \dot{r}^2 = \xi^2 - kg_{\nu\nu}.$$

For a circular orbit, the geodesic equation [20] is also given by  $\ddot{r} = -\frac{mk}{r^2}$ .

Assembling these results, we obtain the equations

$$(3.4) \quad \dot{\nu} = g^{\nu\nu} \left( \xi - \omega \sqrt{\xi^2 - kg_{\nu\nu}} \right)$$

$$(3.5) \quad \dot{r} = \omega \sqrt{\xi^2 - kg_{\nu\nu}},$$

where  $\omega$  has been chosen to represent outgoing geodesics for  $\omega = +1$ , and ingoing geodesics for  $\omega = -1$ . Now, the function of  $r$  that is suitable for our study of geodesics can be inferred:

$$(3.6) \quad \nu(r) = \int \frac{\dot{\nu}}{\dot{r}} dr = \int \frac{g^{\nu\nu} (\xi - \omega \sqrt{\xi^2 - kg_{\nu\nu}})}{\omega \sqrt{\xi^2 - kg_{\nu\nu}}} dr = \int \frac{1}{g_{\nu\nu}} \left( \frac{\omega}{\sqrt{1 - \frac{kg_{\nu\nu}}{\xi^2}}} - 1 \right) dr.$$

In the case of timelike geodesics this gives

$$(3.7) \quad \nu(r) = \int \frac{g^{\nu\nu} (\xi - \omega \sqrt{\xi^2 + g_{\nu\nu}})}{\omega \sqrt{\xi^2 + g_{\nu\nu}}} dr = \int \frac{1}{g_{\nu\nu}} \left( \frac{\omega}{\sqrt{1 + \frac{g_{\nu\nu}}{\xi^2}}} - 1 \right) dr,$$

and for null geodesics we have

$$(3.8) \quad \nu(r) = \int \frac{1}{g_{\nu\nu}} (\omega - 1) dr.$$

For timelike geodesics, the condition  $\omega \sqrt{\xi^2 + g_{\nu\nu}} = 0 \iff \xi^2 + g_{\nu\nu} = 0$ , with the value  $-\xi^2 = g_{\nu\nu}$ , corresponds to the particle either having a turning point or asymptotically approaching a horizon.

These results provide further insights. By renaming the coordinates as  $\nu = \psi$  and  $r = T$ , we can carry over the findings to the Misner case, which takes the same general form as the 2-dimensional cylindrical pseudo-Schwarzschild (4.4) and pseudo-Reissner-Nordström (6.3) spacetimes in Eddington-Finkelstein coordinates:

$$(3.9) \quad ds^2 = f(t)dx^2 + 2dxdt.$$

#### 4. PSEUDO-SCHWARZSCHILD SPACETIME

Although the pseudo-Schwarzschild spacetime is derived from the well-known Schwarzschild spacetime, its global and causal structure more closely resembles that of Misner space. The pseudo-Schwarzschild solution satisfies the Einstein field equations in vacuum and describes a static, hyperbolically symmetric vacuum spacetime [16]. Furthermore, its universal covering space asymptotically approaches Minkowski space, which is known as asymptotic flatness. This serves as another example of a spacetime that violates the chronology condition and allows for the existence of closed timelike curves. The geometry of the pseudo-Schwarzschild spacetime admits a warped product structure, with the base manifold  $S^1 \times \mathbb{R}^+$  and the hyperbolic plane  $H^2$  as the fiber. The point set that defines the pseudo-Schwarzschild manifold is

$$(4.1) \quad M = S^1 \times \mathbb{R}^+ \times H_r^2,$$

where  $S^1$  is the 1-sphere, topologically equivalent to an interval whose endpoints are glued together by identification, and  $H_r^2$  (when  $t, r = \text{const}$ ) represents a 2-dimensional surface that can be identified with

one of the sheets of the two-sheeted space-like hyperboloid.<sup>7</sup> Then the pseudo-Schwarzschild metric can be derived by performing a Wick rotation  $\theta \rightarrow i\theta$  and a signature change from the famous Schwarzschild metric as follows:

$$\begin{aligned}
ds^2 &= -(1 - \frac{2m}{r})dt \otimes dt + (1 - \frac{2m}{r})^{-1}dr \otimes dr + r^2(d\theta \otimes d\theta + \sin^2(\theta)d\phi \otimes d\phi) \\
&\xrightarrow{\theta \rightarrow i\theta} ds^2 = -(1 - \frac{2m}{r})dt^2 + (1 - \frac{2m}{r})^{-1}dr^2 + r^2(d(i\theta)^2 + \underbrace{\sin^2(i\theta)}_{-\sinh^2(\theta)}d\phi^2) \\
&\xrightarrow{(-1)} ds^2 = (1 - \frac{2m}{r})dt^2 - (1 - \frac{2m}{r})^{-1}dr^2 + r^2(d\theta^2 + \sinh^2(\theta)d\phi^2).
\end{aligned}$$

We rewrite the last equation as

$$(4.2) \quad ds^2 = -(\frac{2m}{r} - 1)dt^2 + (\frac{2m}{r} - 1)^{-1}dr^2 + r^2(d\theta^2 + \sinh^2(\theta)d\phi^2),$$

where  $\theta$  takes all positive values,  $0 \leq \phi < 2\pi$ , and  $m \geq 0$ , thereby obtaining the pseudo-Schwarzschild metric. However, in contrast to the Schwarzschild solution, this spacetime exhibits hyperbolic symmetry, and the coordinate  $t$  is assumed to be periodic, with  $0 \leq t < a$ , where the identification  $(t, r, \theta, \phi) \sim (t + na, r, \theta, \phi)$  for  $n \in \mathbb{N}$  is applied. Note that, due to the identification of edge-to-edge points as defined above, there is a change in the topology of the spacetime.

The periodicity of the coordinate  $t$ , after the Wick rotation, arises from the fact that the structure of the corresponding isometry group changes from the non-compact additive group  $\mathbb{R}$  to the compact group  $U(1)$ , which has inherently periodic orbits. In general, the real Lie algebra of the isometry group is generated by the associated Killing vector fields; that is, the infinitesimal generators of one-parameter isometry groups. However, Wick rotating a coordinate (i.e., multiplying it by  $i$ ) changes the associated real Lie algebra into a different real form of a common complexified Lie algebra.

For example, the real Lie algebras of  $\mathbb{R}$  and  $U(1)$  both complexify to the complex Lie algebra  $\mathbb{C}$ , which is the Lie algebra of the complex multiplicative group  $\mathbb{C}^* \setminus \{0\}$ . Thus, the transition between  $\mathbb{R}$  and  $U(1)$  reflects a change in real form within the same complexified structure.

In the specific construction used above, this transformation arises via a *double Wick rotation*:

$$\theta \mapsto i\theta, \quad t \mapsto it.$$

Under this transformation, the isometry group associated with  $\theta$  changes from  $U(1)$  to  $\mathbb{R}$ , while the group associated with  $t$  changes conversely from  $\mathbb{R}$  to  $U(1)$ . Consequently, the new imaginary time coordinate becomes periodic due to the compactness of  $U(1)$ .

---

<sup>7</sup>The upper sheet of the hyperboloid can be globally embedded in 3-dimensional Minkowski space. We can express the upper sheet hyperboloid using a parameterization in polar coordinates  $(\theta, \phi)$ . Specifically, the map  $\mathbb{R}^+ \times S^1 \rightarrow H_r^2$ ,  $(\theta, \phi) \mapsto (r\cosh(\theta), r\sinh(\theta)\cos(\phi), r\sinh(\theta)\sin(\phi))$  describes the embedding of the upper sheet of the hyperboloid in Minkowski space. The hyperboloid together with the induced Riemannian metric  $g = d\theta \otimes d\theta + \sinh^2(\theta)d\phi \otimes d\phi$  is called *hyperbolic plane*.

This periodicity is not merely a formal artifact but carries physical meaning. For instance, imaginary time is also periodic in the Euclidean Schwarzschild solution, where the length of the period corresponds to the inverse of the Hawking temperature of the original black hole. Hence, the periodic nature of imaginary time in the pseudo-Schwarzschild context is consistent with both geometric reasoning and physical interpretation.

Since the geometry of the pseudo-Schwarzschild spacetime can be expressed as a warped product, with the cylindrical base  $M_Z := S^1 \times \mathbb{R}^+$  and the hyperbolic plane  $H^2$  as the fiber, the metric 4.2 can be decomposed into two parts. We introduce coordinates  $(\nu, r)$  on the cylindrical base  $M_Z$ , where  $\nu$  serves as an angular coordinate on  $S^1$  and  $r$  denotes the standard coordinate on  $\mathbb{R}^+$ . The induced cylindrical metric on  $M_Z$  is then given by  $g_z := -(\frac{2m}{r} - 1)d\nu^2 + 2d\nu dr$ , while the metric on the hyperbolic plane  $H^2$  is  $g_{H^2} := d\theta^2 + \sinh^2(\theta)d\phi^2$ , where  $(\theta, \phi)$  are pseudo-spherical polar coordinates.

*Remark.* Considering the universal covering space of the pseudo-Schwarzschild spacetime, we progressively recover flat space as  $r \rightarrow \infty$ . The metric, as given in Equation (4.2), exhibits a pathological behavior at  $r = 2m$  and  $r = 0$ . As we will show later,  $r = 2m$  corresponds to a Cauchy horizon, while  $r = 0$  is a physical singularity analogous to the Schwarzschild singularity. However, there is a key difference: the pseudo-Schwarzschild singularity is timelike, whereas the Schwarzschild singularity is spacelike. This implies that no event inside the horizon can influence any event at  $r > 2m$ . A simple calculation reveals that  $r = 0$  represents a curvature singularity, whereas the point  $r = 2m$  is merely a coordinate singularity. Later, we will introduce appropriate coordinates that eliminate the coordinate singularity.

The pseudo-Schwarzschild spacetime is static inside the horizon and time-dependent outside of the horizon. For  $r < 2m$ , the  $t$ -direction  $\partial_t$  is timelike, and  $r$  is a spatial coordinate and the  $r$ -direction  $\partial_r$  is spacelike, as seen from the metric components:

$$g_{tt} = -\left(\frac{2m}{r} - 1\right) < 0$$

$$g_{rr} = \left(\frac{2m}{r} - 1\right)^{-1} > 0.$$

However, beyond the horizon,  $r > 2m$ , there is a reversal of the roles:  $t$  becomes a spatial coordinate and  $r$  becomes a timelike coordinate. In this region, the decrease of  $r$  signifies the passage of time. As long as you remain in the region  $r > 2m$ , you are inevitably moving forward in time and will hit the horizon at  $r = 2m$ . All trajectories lead inevitably to the horizon. Once you cross the horizon, the roles of  $t$  and  $r$  are effectively switched, with  $t$  becoming a timelike coordinate and  $r$  a spatial one.<sup>8</sup> Analogous to the Schwarzschild metric, the pseudo-Schwarzschild metric has a horizon at  $r = 2m$  and a singularity occurs at  $r = 0$ . As discussed earlier, the issue with our current coordinates becomes apparent along radial null geodesics, where the slope  $\frac{dt}{dr}$  diverges as  $r$  converges towards  $2m$ , i.e.  $\frac{dt}{dr} \rightarrow \infty$ .

To eliminate the coordinate singularity at  $r = 2m$ , we can convert the pseudo-Schwarzschild coordinates into Eddington-Finkelstein coordinates. Similar to the Schwarzschild case, we set the term  $r + 2m \ln |r - 2m|$

---

<sup>8</sup>We can analyze the behavior of radial null curves by setting  $d\theta = d\phi = 0$  and studying the equation  $dt = \pm \frac{1}{(\frac{2m}{r}-1)} dr$ . For large  $r$ , the slope is  $\frac{dt}{dr} = \pm 1$ , which is consistent with the behavior in flat space. As we approach  $r = 2m$ , we get  $\frac{dt}{dr} = \pm \infty$  meaning that the light cones close up at this point. Further, as we approach the singularity at  $r = 0$ , the light cones are stretched again, but are tilted according to their reversed role of  $t$  and  $r$  as timelike and spacelike coordinates.

equal to the tortoise coordinate  $r^*$ . Then, we set  $\nu = -(t + r^*)$ , which leads to the inverse relationship  $t = -(\nu + r + 2m \ln |r - 2m|)$ . Next, we take the derivative of this equation  $dt = -d(\nu + r + 2m \ln |r - 2m|)$ , and square both sides. By substituting this expression for  $dt^2$  into the pseudo-Schwarzschild metric, we obtain the following form of the metric in terms of the tortoise coordinate

$$(4.3) \quad ds^2 = -\left(\frac{2m}{r} - 1\right)d\nu^2 + 2d\nu dr + r^2(d\theta^2 + \sinh^2(\theta)d\phi^2).$$

The new coordinate  $\nu$  is periodic, with  $0 \leq \nu < \beta$ , similar to the previous coordinate  $t$ . A given point  $(0, r, \theta, \phi)$  is identified with  $(b, r, \theta, \phi)$ , where  $b$  is the periodicity of the coordinate  $\nu$ . These coordinates are naturally adapted to the null geodesics. Although the metric component  $g_{\nu\nu}$  disappears at  $r = 2m$ , the coordinate transformation eliminates the singularity that existed at  $r = 2m$  in the original pseudo-Schwarzschild coordinates. Moreover, the null hypersurface at  $r = 2m$  serves as a Cauchy horizon, denoted  $H$ , and divides the spacetime  $M$  into two regions:  $M_2$ , where  $r < 2m$ , and  $M_1$ , where  $r > 2m$ . We can time-orient the manifold  $M$  by requiring that  $-\partial_r$  be future-pointing. This leads to the conclusion that  $\partial_r$  is a lightlike vector throughout,  $\partial_\nu$  is timelike for  $r < 2m$ , and spacelike for  $r > 2m$ .

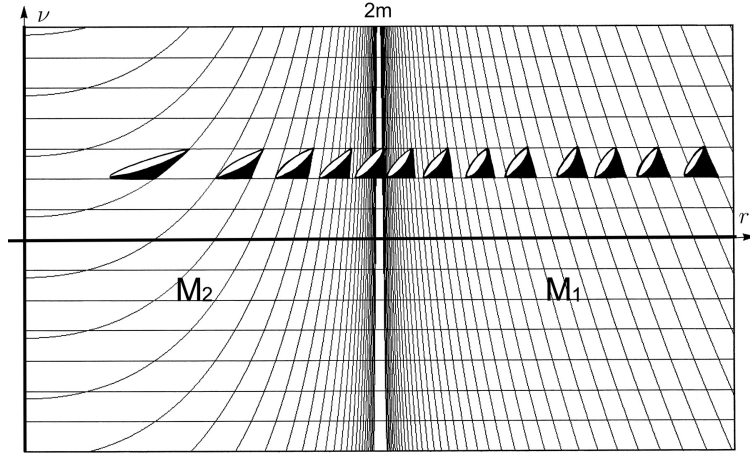


FIGURE 6. Pseudo-Schwarzschild spacetime in Eddington-Finkelstein coordinates.

Recalling that the pseudo-Schwarzschild spacetime is  $M = M_Z \times_r H^2$ , and its metric can be decomposed into the cylindrical metric  $g_Z$  and the hyperbolic metric  $g_{H^2}$ , we proceed by setting  $\theta = \text{const}$  and  $\phi = \text{const}$ . Allowing  $\nu$  and  $r$  to vary and take the values as previously defined, we obtain the 2-dimensional cylindrical pseudo-Schwarzschild spacetime  $M_Z = S^1 \times \mathbb{R}^+$ . This spacetime is described by the degenerate metric in Eddington-Finkelstein coordinates (see Figure 6):

$$(4.4) \quad g_Z := -\left(\frac{2m}{r} - 1\right)d\nu^2 + 2d\nu dr.$$

In two dimensions, the Christoffel symbols are identical for both the Schwarzschild and pseudo-Schwarzschild spacetimes. Therefore, the Riemann curvature tensor for the cylindrical pseudo-Schwarzschild spacetime (4.3) is given by  $-R_{ttrr} = -\frac{2m}{r^3} =: K = \frac{1}{2}S$ , where  $K$  denotes the Gaussian curvature and  $S$  represents the scalar

curvature. Since we require  $m$  to be non-negative and  $r$  to be positive, the Gaussian curvature is non-positive throughout the cylinder.<sup>9</sup>

**4.1. Non-chronal region.** In cylindrical coordinates  $(\nu, r)$ , the  $\nu$ -coordinate curves circle around the cylinder. Given the metric in Eddington-Finkelstein coordinates (as presented in Equation 4.4), besides  $\theta, \phi$ , we can also set  $r$  to a constant value and consider the one-dimensional line element

$$g_{\bar{Z}} = -\left(\frac{2m}{r} - 1\right)d\nu^2.$$

The curves  $\gamma : [0, b] \rightarrow M$ , defined by  $\gamma(s) = (s, r, \theta, \phi)$ , are closed because  $\gamma(0) = (0, r, \theta, \phi) = (b, r, \theta, \phi) = \gamma(b)$ . Since each curve is contained within a hypersurface of constant  $r = \text{const}$  and is equipped with the metric  $g_{\bar{Z}}$ , the nature of the curves depends on the value of  $r$ : the curves are timelike if and only if  $r < 2m$ , the curves are spacelike if  $r > 2m$ . At  $r = 2m$ , the horizon  $H$  is null and consists of closed null curves  $\gamma(s) = (s, 2m, \theta, \phi)$ , where  $\theta$  and  $\phi$  are constant. Therefore,  $H$  serves as a chronology horizon for the closed orbits of constant  $r, \theta, \phi$ .

**Proposition 4.1.** *A curve  $\gamma : I \rightarrow M_z$  with velocity  $\gamma' = \gamma'_1 \partial_\nu + \gamma'_2 \partial_r$  is causal and future-pointing in  $M_1$  if and only if  $0 \leq \frac{2 \cdot \gamma'_2}{\left(\frac{2m}{r} - 1\right)} \leq \gamma'_1$ , and is causal and future-pointing in  $M_2$  if and only if  $\frac{2 \cdot \gamma'_2}{\left(\frac{2m}{r} - 1\right)} \geq \gamma'_1 \geq 0$ .*

*Proof.* We will not go into the details here, as the proof follows a similar structure to that of Lemma 6.2, where we discuss the properties of the pseudo-Reissner-Nordström spacetime.  $\square$

**Proposition 4.2.** *There are no closed timelike curves in the region  $M_1 \subset M_Z$ .*

*Proof.* We begin by considering a foliation of  $M_Z$  using the hypersurfaces  $\mathcal{H}_r := \{(\nu, r) \mid 0 \leq \nu \leq 2\pi\}$  where  $r = \text{const}$ . The hypersurfaces  $\mathcal{H}_r$  are spacelike for  $r > 2m$ , thus we have  $M_1 = \bigcup_{r \in (2m, \infty)} \mathcal{H}_r$ . Given that any curve in this region must be future-pointing, a curve in  $M_1$  can only close up if it is contained within a circle in  $\mathcal{H}_r$ , i.e., if the curve is spacelike and satisfies the condition  $r = \text{const}$ . This is the only way for the curve to be periodic and contained within a single hypersurface  $\mathcal{H}_r$ . Therefore, such curves are spacelike.  $\square$

The absence of closed timelike curves in region  $M_1$  implicates that all closed timelike curves must be part of region  $M_2$ .

**4.2. Pseudo-Schwarzschild geodesics.** The timelike geodesics for the pseudo-Schwarzschild spacetime in Eddington-Finkelstein coordinates are given by Equation (3.7), using the relation  $g_{\nu\nu} = -\left(\frac{2m}{r} - 1\right)$ :

$$(4.5) \quad \nu(r) = \int \frac{-\frac{1}{\left(\frac{2m}{r} - 1\right)} \left(\xi - \omega \sqrt{\xi^2 - \left(\frac{2m}{r} - 1\right)}\right)}{\omega \sqrt{\xi^2 - \left(\frac{2m}{r} - 1\right)}} dr = \int \frac{-1}{\left(\frac{2m}{r} - 1\right)} \left( \frac{\omega}{\sqrt{1 - \frac{\left(\frac{2m}{r} - 1\right)}{\xi^2}}} - 1 \right) dr.$$

There are two distinct sets of timelike geodesics in the pseudo-Schwarzschild spacetime. The first set corresponds to a timelike particle that penetrates the chronology horizon at  $r = 2m$ . This particle has a turning point at

<sup>9</sup>The Riemannian curvature tensor for the 4-dimensional pseudo-Schwarzschild spacetime can easily be computed by the prescription of Wick rotation and sign change.

$$r_{turn} = \frac{2m}{(\xi^2 + 1)},$$

which lies between the singularity and the chronology horizon. As a result, such a massive particle cannot reach the singularity. The second set of geodesics corresponds to a particle that spirals around the horizon as it approaches  $r = 2m$ , but it never crosses the horizon within this coordinate patch. For photons, the paths are determined by the equation

$$\nu(r) = \int \frac{-1}{\left(\frac{2m}{r} - 1\right)} (\omega - 1) dr.$$

Curiously, there is no obstruction for photons to fall into the singularity.

## 5. RELATION BETWEEN PSEUDO-SCHWARZSCHILD AND MISNER SPACETIME

We aim to investigate Misner space and the 2-dimensional pseudo-Schwarzschild spacetime  $(M_Z, g_Z)$ , focusing on similarities such as global causal structure, curvature, and geodesics. In addition to these, the conformal structure of these spacetimes is notably rich. A conformal transformation can sometimes convert a curved space with a non-zero Riemann tensor into a flat space with a zero Riemann tensor. However, depending on the dimension of the spacetime, a less strict concept of causal relatedness may be required. In this context, we introduce the concept of isocausality [6], which refers to a situation where the causal structure of spacetime may not be preserved globally under certain transformations, but the notion of causal relationships within specific regions remains consistent.

A glance at the causal structure of the cylindrical pseudo-Schwarzschild space and the 2-dimensional Misner space might suggest that the two associated metrics, metric (4.4) and the 2-dimensional variant of metric (2.4), are related. This raises the natural question of whether an isometric mapping exists between these manifolds. However, it is known that any isometry of a pseudo-Riemannian manifold preserves its curvature. Since the Riemann curvature vanishes in Misner space, but does not vanish in the cylindrical pseudo-Schwarzschild space, no isometry exists between them.

*Remark 5.1.* It is worth noting that in the special case  $m = 0$ , the 2-dimensional pseudo-Schwarzschild spacetime is defined on  $S^1 \times \mathbb{R}$  and is flat. However, by setting  $m = 0$ , the chronology horizon in the pseudo-Schwarzschild space disappears, and closed timelike curves (CTCs) no longer exist. This distinction makes these spacetimes causally different, as the chronology horizon is a significant global feature that separates the chronology-violating region from the region without CTCs. In what follows, we will restrict our investigation to the case where  $m > 0$ .

**5.1. General case.** For radial trajectories in hyperbolically symmetric spacetimes, the geometry is effectively 1+1 dimensional. Therefore, for simplicity and ease of calculation, we first focus on the 2-dimensional Misner space and the cylindrical pseudo-Schwarzschild space, as these lead to relatively straightforward conformal transformations. Afterward, we turn our attention to 4-dimensional spacetimes, although the results from the 2-dimensional case cannot be directly generalized. This gives rise to an alternative perspective on causal equivalence, as introduced by [6]. This approach allows for the consideration of a much larger class of causally related spacetimes compared to the classical concept of conformally related spacetimes.

5.1.1. *Relation in the two-dimensional case.* Since the metrics under study are 2-dimensional, we know that both metrics in question belong to the same conformal equivalence class  $[g]$  of conformally flat metrics.<sup>10</sup> Hence, if the metrics  $g_P, g_M \in [g]$  are both locally conformal to a flat metric  $g$ , i.e.  $(g_M \sim g) \wedge (g_P \sim g)$ , then by transitivity and symmetry we have  $g_P \sim g_M$ . As a result, we can locally transform the curved pseudo-Schwarzschild space with a non-vanishing Riemann tensor into the flat Misner space with a zero Riemann tensor by applying a conformal transformation.

Consider the 2-dimensional flat Misner space defined on  $S^1 \times \mathbb{R}$  and equipped with the metric

$$(5.1) \quad ds^2 = Td\varphi^2 - dTd\varphi.$$

*Remark 5.2.* This version of Misner metric can be obtained from the 2-dimensional Minkowski metric (2.1) by the initial coordinate transformation  $\tilde{t} = \eta \cosh(X_1)$  and  $\tilde{x}_1 = \eta \sinh(X_1)$ . This coordinate change results in the Misner metric  $ds^2 = -d\eta^2 + \eta^2(dX_1)^2$ , where  $0 < \eta < \infty$ ,  $0 \leq X_1 \leq 2\pi$ . Another coordinate change with  $\varphi = X_1 + \ln(\eta)$  and  $T = \eta^2$  results in the Misner metric  $-dTd\varphi + Td\varphi^2$ , where the domains are  $-\infty < T < \infty$  and  $0 \leq \varphi \leq 2\pi$ .

The pseudo-Schwarzschild spacetime is defined on  $S^1 \times (0, \infty)$ , with the corresponding line-element

$$(5.2) \quad ds^2 = -\left(\frac{2m}{r} - 1\right)d\nu^2 + 2d\nu dr.$$

Obviously the base manifolds are diffeomorphic. We start with Equation (5.2). For convenience, we introduce dimensionless quantities  $\bar{r} = \frac{r}{m}$ ,  $\bar{t} = \frac{t}{m}$  and rewrite the metric ((5.2)) as

$$\begin{aligned} ds^2 &= -\left(\frac{2}{\bar{r}} - 1\right)d(\bar{\nu}m)^2 + 2d(\bar{\nu}m)d(\bar{r}m) \\ &= m^2\left[-\left(\frac{2}{\bar{r}} - 1\right)d\bar{\nu}^2 + 2d\bar{\nu}d\bar{r}\right] \\ &= m^2\left(\frac{2}{\bar{r}} - 1\right)\left[-d\bar{\nu}^2 + \underbrace{2\left(\frac{2}{\bar{r}} - 1\right)^{-1}d\bar{r}d\bar{\nu}}_{d(r^*)}\right]. \end{aligned}$$

Next we introduce

$$(5.3) \quad d(r^*)^2 := 2\left(\frac{2}{\bar{r}} - 1\right)^{-1}d\bar{r},$$

with  $r^* = -2(\bar{r} + 2 \log(\bar{r} - 2))$ . This implies the line-element

$$ds^2 = m^2\left(\frac{2}{\bar{r}} - 1\right)\left[-d\bar{\nu}^2 + d(r^*)d\bar{\nu}\right].$$

We then redefine both coordinates as  $\varphi = \alpha\bar{\nu}$  and  $T = e^{\alpha r^*}$ , where  $\alpha$  is an arbitrary constant. Considering that  $r^* = \frac{1}{\alpha} \cdot \log(T)$  yields

$$d\bar{\nu} = d\frac{\varphi}{\alpha} = \frac{1}{\alpha}d\varphi$$

---

<sup>10</sup>A metric is said to be conformally flat if it can be conformally transformed into a metric with vanishing Riemann curvature.

and

$$d(r^*) = d\left(\frac{1}{\alpha} \cdot \log(T)\right) = \frac{1}{\alpha T} dT.$$

With these expressions we obtain as line-element

$$\begin{aligned} ds^2 &= m^2\left(\frac{2}{\bar{r}} - 1\right)\left[-\left(\frac{1}{\alpha} d\varphi\right)^2 + \left(\frac{1}{\alpha T} dT\right)\left(\frac{1}{\alpha} d\varphi\right)\right] \\ &= m^2\left(\frac{2}{\bar{r}} - 1\right)\left[-\frac{1}{\alpha^2} d\varphi^2 + \frac{1}{\alpha^2 T} dT d\varphi\right]. \end{aligned}$$

By multiplication with  $(-1)$  we get

$$\begin{aligned} ds^2 &= -m^2\left(\frac{2}{\bar{r}} - 1\right)\frac{1}{\alpha^2} \frac{1}{T} [-Td\varphi^2 + dTd\varphi] = \underbrace{\left(\frac{2}{\bar{r}} - 1\right)\frac{m^2}{T\alpha^2}}_{\Omega(T)} [-dTd\varphi + Td\varphi^2] \\ &= \Omega(T)[-dTd\varphi + Td\varphi^2]. \end{aligned}$$

The conformal factor  $\Omega$  is singular at the original horizon  $r = 2m$ . However, to ensure that the conformal factor is non-zero, we set the following expression for  $T$  (based on the defined terms above):

$$T = e^{\alpha r^*} = e^{\alpha(-2\bar{r} - 4 \log(\bar{r} - 2))} = e^{-2\alpha\bar{r}} \cdot e^{-\alpha 4 \log(2 - \bar{r})} = e^{-2\alpha\bar{r}} \cdot (2 - \bar{r})^{-4\alpha}.$$

Hence,

$$\begin{aligned} \Omega(\bar{r}) &= \left(\frac{2}{\bar{r}} - 1\right) \frac{m^2}{\alpha^2 (e^{-2\alpha\bar{r}} \cdot (2 - \bar{r})^{-4\alpha})} = \frac{m^2}{\bar{r}\alpha^2} (2 - \bar{r}) \frac{1}{(2 - \bar{r})^{-4\alpha}} \cdot e^{2\alpha\bar{r}} \\ &= \frac{m^2}{\bar{r}\alpha^2} (2 - \bar{r}) (2 - \bar{r})^{4\alpha} \cdot e^{2\alpha\bar{r}} = \frac{m^2 e^{2\alpha\bar{r}}}{\bar{r}\alpha^2} (2 - \bar{r})^{4\alpha+1}, \end{aligned}$$

and we choose  $\alpha = -\frac{1}{4}$  to make  $\Omega$  regular on the chronology horizon, e.g. to ensure  $\Omega \neq 0$ . Going back to the original coordinates, we have

$$\Omega(r) = \frac{m^2 e^{\frac{-r}{2m}}}{\frac{r}{16m}} \left(2 - \frac{r}{m}\right)^0 = \frac{16m^3 e^{\frac{-r}{2m}}}{r}$$

for the conformal factor. Furthermore, we rewrite the conformal factor in terms of the actual coordinates  $T$ ,  $\varphi$ . Note that  $r = \bar{r}m = 2m \left(W_n\left(-\frac{T}{2e}\right) + 1\right)$ ,  $n \in \mathbb{Z}$ , where the expression  $W$  is the *product log* function. Replacing  $r$  by  $2m \left(W\left(-\frac{T}{2e}\right) + 1\right)$  yields the conformal factor

$$\begin{aligned} \Omega(T) &= \frac{16m^3 e^{\frac{-r}{2m}}}{r} = \frac{16m^3 e^{-\frac{2m \left(W\left(-\frac{T}{2e}\right) + 1\right)}{2m}}}{2m \left(W\left(-\frac{T}{2e}\right) + 1\right)} = \frac{8m^2 e^{-\left(W\left(-\frac{T}{2e}\right) + 1\right)}}{\left(W\left(-\frac{T}{2e}\right) + 1\right)} \\ &= \frac{8m^2 e^{-\left(W\left(-\frac{T}{2e}\right) + 1\right)}}{W\left(-\frac{T}{2e}\right) + 1} = \frac{8m^2}{e^{\left(W\left(-\frac{T}{2e}\right) + 1\right)} \cdot W\left(-\frac{T}{2e}\right) + 1} = \frac{8m^2}{e^{\left(W\left(-\frac{T}{2e}\right) + 1\right)} - \frac{T}{2}} \end{aligned}$$

and the corresponding line-element

$$ds^2 = \frac{8m^2}{\underbrace{e^{(W(-\frac{T}{2c})+1) - \frac{T}{2}}}_{\Omega(T)}} [-dTd\varphi + Td\varphi^2],$$

where the conformal factor,  $\Omega(T)$ , is a smooth, non-zero scalar function of the spacetime coordinates. Conformal transformations preserve the local causal structure: they map timelike curves to timelike curves, spacelike curves to spacelike curves, and null curves to null curves. Furthermore, we have the well-known

**Proposition 5.3.** *Conformal transformations between 2-dimensional Lorentzian manifolds send null hypersurfaces to null hypersurfaces and therefore null geodesics to null geodesics.*

However, timelike geodesics in one spacetime are not necessarily geodesics in another conformally equivalent spacetime, even if both spacetimes are related by a conformal diffeomorphism. Nonetheless, the treatments of timelike geodesics in Equation 2.2 and Equation 4.2 demonstrate that the geodesic behavior in both spacetimes is, in fact, similar.

This means that for the 1 + 1 dimensional pseudo-Schwarzschild and Misner spacetimes, we can identify conformal transformations and demonstrate that timelike geodesics are of a similar type in both spacetimes. This establishes a notable relationship between them, with the 2-dimensional pseudo-Schwarzschild spacetime being viewed as a modification or generalization of Misner space. However, the 4-dimensional pseudo-Schwarzschild solution is not conformally flat, as indicated by the non-zero components of the conformally invariant Weyl tensor. In fact, only one independent spin component of the Weyl tensor does not vanish, specifically the Weyl scalar  $C = \frac{m}{r^3}$ . Therefore, in this context, a less strict definition of causal relatedness is required.

5.1.2. *Relation in the 4-dimensional case.* Since the Weyl curvature tensor vanishes identically in two dimensions, all 2-dimensional Lorentz metrics belong to the same conformal class of flat metrics. Therefore, it is relatively straightforward to find conformal transformations between any two representatives of this conformal class. In dimensions greater than three, the Weyl curvature tensor is generally non-zero, and a necessary condition for a spacetime to be conformally flat is that the Weyl tensor vanishes. As a result, establishing an explicit conformal relation between 4-dimensional spacetimes becomes significantly more challenging.

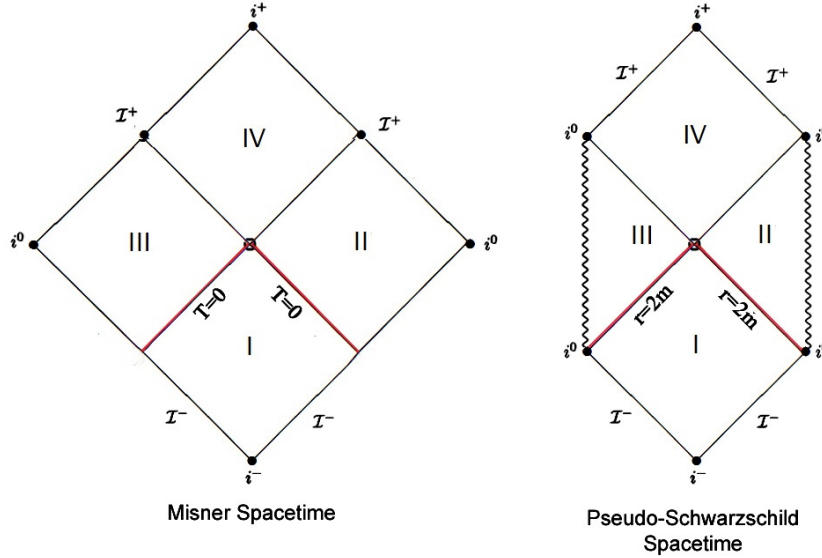


FIGURE 7. Conformal diagrams for the coverings spaces of Misner space and pseudo-Schwarzschild spacetime. The resemblance is noteworthy and we suspect a causal relationship. According to [6], Penrose diagrams are very helpful to get a clearer picture of the large-scale structure and to detect isocausality.

In four dimensions, Misner space is flat, while pseudo-Schwarzschild spacetime is not conformally flat. Therefore, these two spacetimes do not belong to the same conformal class. At this point, we turn to the concept of causal relations, known as isocausality, which is more general than conformal relations. We consider mappings that preserve causal relations, even if their inverses do not necessarily do so. This notion was proposed by García-Parrado and Senovilla [6] and further developed by A. García-Parrado and M. Sánchez [7]. The analogy between the pseudo-Schwarzschild and Misner spacetimes becomes clearer through Penrose diagrams, as shown in Figure 7. These diagrams reveal that the universal covering spaces of these spacetimes share the same large-scale structure.

*Remark 5.4.* The boundaries in the diagram are not part of the original spacetimes. It is important to remember that we imposed periodicity on one coordinate in the original spacetimes, which cannot be appropriately represented in the Penrose diagrams.

Ultimately, these results lead us to the following

**Conjecture 5.5.** *The 4-dimensional pseudo-Schwarzschild spacetime and Misner space are isocausal.*

## 6. PSEUDO-REISSNER-NORDSTRÖM SPACETIME

We begin with the well-known Reissner-Nordström spacetime and modify it to create a novel spacetime, which we refer to as the pseudo-Reissner-Nordström spacetime. The two metrics are related through Wick rotation and a change in signature. Comprehensive references for the Reissner-Nordström spacetime include [2, 11, 15]. Our focus will be on the geometry of the newly derived pseudo-Reissner-Nordström spacetime, examining its global structure, geodesics, and causal properties. Furthermore, we will explore how this

spacetime relates to the pseudo-Schwarzschild and Misner spacetimes, with many of the properties we derive also applying to these two spacetimes.

By performing a Wick rotation  $\theta \rightarrow i\theta$  on the Reissner-Nordström metric, changing the range of  $\theta$  from  $[0, \pi]$  to  $[0, +\infty]$ , flipping the signature, and identifying  $t + P$  with  $t$ , we obtain the manifold

$$M := S^1 \times (0, \infty) \times H_r^2,$$

with coordinates  $(t, r, \theta, \varphi)$ , equipped with the metric

$$(6.1) \quad ds^2 = -\left(\frac{2m}{r} - \frac{q^2}{r^2} - 1\right)dt^2 + \left(\frac{2m}{r} - \frac{q^2}{r^2} - 1\right)^{-1}dr^2 + r^2(d\theta^2 + \sinh^2(\theta)d\phi^2).$$

Similar to the pseudo-Schwarzschild manifold, the 1-sphere  $S^1$  (with  $0 \leq t < t + \alpha$ ) is topologically equivalent to an interval with its endpoints identified. The surface  $H_r^2$  is 2-dimensional and corresponds to the upper sheet of a two-sheeted spacelike hyperboloid. The coordinate  $\theta$  can take any positive value, while  $\phi$  is periodic and ranges from  $0 \leq \phi < 2\pi$ . The real constants  $m$  and  $q$  represent mass and electric charge, respectively, and are assumed to be positive. This new metric can also be derived by performing a Wick rotation and a signature change on the Schwarzschild metric, followed by the substitution

$$m \rightarrow m(r) := m - \frac{q^2}{2r},$$

which reduces back to the pseudo-Schwarzschild metric when  $q = 0$ . The metric, as given in Equation (5), is singular when

$$\frac{2m}{r} - \frac{q^2}{r^2} - 1 = 0 \iff r_{\pm} = m \pm \sqrt{m^2 - q^2},$$

and also at  $r = 0$ .

The singularities at  $r = r_-$  and  $r = r_+$  are not true physical singularities; rather, they represent quasi-regular singularities arising from geodesic incompleteness.

*Remark.* In the case of the Reissner-Nordström spacetime, matter is present—at least in the form of an electrostatic field—so it is not a vacuum solution of Einstein’s field equations. A vacuum solution requires both the Einstein tensor and the stress-energy tensor to vanish identically, meaning that no matter or non-gravitational fields are present. In contrast, the Reissner-Nordström solution includes a non-zero electromagnetic field, which contributes to the stress-energy tensor. As such, it is classified as an *electrovacuum* solution of the Einstein–Maxwell equations, where the electromagnetic field is sourced by a vector potential. In mathematical terms, when the Reissner-Nordström metric is written with signature  $(-+++)$ , it satisfies Einstein’s equations in the form  $R_{\mu\nu} - \frac{1}{2}Rg_{\mu\nu} = \kappa T_{\mu\nu}$ , where  $T_{\mu\nu}$  is the energy–momentum tensor associated with the corresponding electromagnetic field.

Our construction of the pseudo-Reissner-Nordström spacetime involves performing a Wick rotation on the angular coordinate,  $\theta \rightarrow i\theta$ , resulting in a hyperbolic geometry in the angular sector. This transformation leaves the time coordinate unchanged, and the electromagnetic field strength  $F = dA$  formally retains its original expression. However, in our construction, the Wick rotation is followed by a sign reversal of the

metric. This change flips the sign on the right-hand side of the Einstein field equations while leaving the left-hand side invariant. Specifically, if we first apply the transformation  $\theta \rightarrow i\theta$ , and then reverse the overall sign of the metric, we once again obtain a Lorentzian metric with signature  $(-+++)$ , but differing from the original by an overall sign. Under this transformation, the field strength  $F_{\mu\nu}$  remains unchanged, while the mixed-index version  $F_{\mu}{}^{\nu}$  acquires a minus sign. Similarly, the contraction  $g_{\mu\nu}F_{\alpha\beta}F^{\alpha\beta}$  changes sign. As a result, the right-hand side of the Einstein field equations changes sign, while the left-hand side remains the same.

Consequently, the resulting spacetime is no longer a solution of the Einstein–Maxwell equations. The energy–momentum tensor corresponding to the pseudo-Reissner-Nordström metric violates the weak energy condition: the gravitational source now corresponds to a form of ‘exotic matter’ with negative energy density. This situation differs significantly from the case of the pseudo-Schwarzschild metric, where the original stress-energy tensor was zero—and remains zero after the transformation. The pseudo-Schwarzschild metric, therefore, remains a valid vacuum solution to Einstein’s equations, whereas the pseudo-Reissner-Nordström metric is no longer a solution of the Einstein–Maxwell equations. This distinction is critical because it differentiates the pseudo-Reissner-Nordström spacetime from the Misner and pseudo-Schwarzschild spacetimes, both of which are vacuum solutions. What makes the pseudo-Reissner-Nordström spacetime particularly surprising and significant as a member of the causality-violating spacetime family is its non-vacuum character.

Before discussing causality, we will change coordinates and define the extended manifold. There exists a set of coordinates that better describe the singularities at  $r = r_-$  and  $r = r_+$ . To achieve this, we introduce the Eddington-Finkelstein coordinates  $(\nu, r, \theta, \phi)$ , which can be introduced as follows:

We regard  $\theta$  and  $\phi$  being constant and first compute the tortoise coordinate  $r^*$  by setting

$$ds^2 = -\left(\frac{2m}{r} - \frac{q^2}{r^2} - 1\right)dt^2 + \frac{1}{-\left(\frac{2m}{r} - \frac{q^2}{r^2} - 1\right)}dr^2 = 0.$$

We can now assert that

$$\frac{dt^2}{dr^2} = \frac{1}{\left(\frac{2m}{r} - \frac{q^2}{r^2} - 1\right)^2} \implies \frac{dt}{dr} = \pm \frac{1}{\left(\frac{2m}{r} - \frac{q^2}{r^2} - 1\right)}.$$

Then we integrate  $\frac{dt}{dr} = \frac{1}{\left(\frac{2m}{r} - \frac{q^2}{r^2} - 1\right)}$  to obtain

$$\begin{aligned} t(r) &= \int \frac{1}{\left(\frac{2m}{r} - \frac{q^2}{r^2} - 1\right)} dr \\ &= (2m^2 - q^2) \cdot \tan^{-1}\left(\frac{r-m}{\sqrt{q^2 - m^2}}\right) - m \cdot \log(-2mr - q^2 + r^2) - r + c, \end{aligned}$$

which yields the tortoise coordinate which is defined by

$$r^* := (2m^2 - q^2) \cdot \tan^{-1}\left(\frac{r-m}{\sqrt{q^2 - m^2}}\right) - m \cdot \log(-2mr - q^2 + r^2) - r.$$

Thus, we obtain the Eddington-Finkelstein coordinates  $\nu = t + r^*$ . Our next step is to express the pseudo-Reissner-Nordström metric in terms of the tortoise coordinate. We define  $t = \nu - r^*$  and substitute  $t$  with the term  $\nu - r^*$  in the original metric (6.1):

$$\begin{aligned}
ds^2 &= -\left(\frac{2m}{r} - \frac{q^2}{r^2} - 1\right) (d(\nu - r*))^2 + \left(\frac{2m}{r} - \frac{q^2}{r^2} - 1\right)^{-1} dr^2 + r^2(d\theta^2 + \sinh^2(\theta)d\phi^2) \\
&= -\left(\frac{2m}{r} - \frac{q^2}{r^2} - 1\right) \left( \underbrace{\frac{\partial(\nu - r*)}{\partial r}}_{\left(\frac{2m}{r} - \frac{q^2}{r^2} - 1\right)^{-1}} dr + \underbrace{\frac{\partial(\nu - r*)}{\partial \nu}}_1 d\nu \right)^2 \\
&\quad + \left(\frac{2m}{r} - \frac{q^2}{r^2} - 1\right)^{-1} dr^2 + r^2(d\theta^2 + \sinh^2(\theta)d\phi^2) \\
&= -\left(\frac{2m}{r} - \frac{q^2}{r^2} - 1\right) \left[ \left(\frac{1}{\left(\frac{2m}{r} - \frac{q^2}{r^2} - 1\right)^2}\right) dr^2 - 2 \cdot 1 \cdot \frac{1}{\left(\frac{2m}{r} - \frac{q^2}{r^2} - 1\right)} dr d\nu + 1 d\nu^2 \right] \\
&\quad + \left(\frac{2m}{r} - \frac{q^2}{r^2} - 1\right)^{-1} dr^2 + r^2(d\theta^2 + \sinh^2(\theta)d\phi^2) \\
&= -\left(\frac{2m}{r} - \frac{q^2}{r^2} - 1\right)^{-1} dr^2 + 2drd\nu - \left(\frac{2m}{r} - \frac{q^2}{r^2} - 1\right) d\nu^2 \\
&\quad + \left(\frac{2m}{r} - \frac{q^2}{r^2} - 1\right)^{-1} dr^2 + r^2(d\theta^2 + \sinh^2(\theta)d\phi^2) \\
&= -\left(\frac{2m}{r} - \frac{q^2}{r^2} - 1\right) d\nu^2 + 2drd\nu + r^2(d\theta^2 + \sinh^2(\theta)d\phi^2).
\end{aligned}$$

Hence, in terms of the Eddington-Finkelstein coordinates, the metric takes the form

$$(6.2) \quad ds^2 = -\left(\frac{2m}{r} - \frac{q^2}{r^2} - 1\right) d\nu^2 + 2drd\nu + r^2(d\theta^2 + \sinh^2(\theta)d\phi^2),$$

where  $\nu$  has the same periodicity as  $t$ . The metric is now regular at  $r = r_-$  and  $r = r_+$ , but we still have an irremovable singularity at  $r = 0$ . Fortunately, the first two terms are independent of the coordinates  $\theta$  and  $\phi$ . To align the pseudo-Reissner Nordström spacetime with the other examples discussed in this article, and because most of our calculations only apply to the coordinates  $\nu$  and  $r$ , we can ignore the term  $r^2(d\theta^2 + \sinh^2(\theta)d\phi^2)$ . From now on we treat  $\theta$  and  $\phi$  as constants and consider the cylindrical metric

$$(6.3) \quad ds^2 = -\left(\frac{2m}{r} - \frac{q^2}{r^2} - 1\right) d\nu^2 + 2drd\nu,$$

with  $\nu$  being periodic with period  $\alpha$ , i.e., the metric is defined on  $M := S^1 \times (0, \infty)$ . Although we have removed the coordinate singularities, the light cones still tilt over at  $r = r_{\pm}$ , as we will discuss later. The horizon function  $H(r)$  given by

$$H(r) = \frac{2m}{r} - \frac{q^2}{r^2} - 1$$

determines the horizons at  $r = r_{\pm}$ . In contrast to the pseudo-Schwarzschild spacetime, there are three distinct cases:

(i) For  $m > q$ , there are two horizons: The event horizon, which is also a Cauchy horizon, at

$$r = r_- = m - \sqrt{m^2 - q^2},$$

and a Cauchy horizon at

$$r = r_+ = m + \sqrt{m^2 - q^2}.$$

Above all, both horizons are chronology horizons.

(ii) For  $m = q$ , there is single horizon at

$$r = r_+ = r_- = m = q,$$

which serves as both a Cauchy horizon and an event horizon.

(iii) For  $m < q$ , no horizon exists, which in the Reissner-Nordström spacetime results in a *naked singularity* observable from the outside. Although an event horizon is absent, the future singularity at  $r = 0$  remains spacelike and thus remains hidden from external observers. This scenario parallels the pseudo-Schwarzschild solution with negative mass, a topic we will not explore further here.

The Riemann curvature tensor for the 2-dimensional pseudo-Reissner-Nordström spacetime can be obtained using the same approach as in Section 4 for the pseudo-Schwarzschild case. The scalar curvature then follows immediately

$$S = g^{jl} Ric_{jl} = \sum_{jl} g^{jl} Ric_{jl} = -2 \cdot \frac{2mr - 3q^2}{r^4}.$$

Thus, the Gaussian curvature  $K$  is given by

$$K = \frac{1}{2}S = -\frac{2mr - 3q^2}{r^4} = -R_{1212}.$$

This result confirms that the Gaussian curvature changes sign based on the value of  $r$ : for  $r < \frac{3q^2}{2m}$ , we find  $2mr - 3q^2 < 0$ , making the Gaussian curvature  $K > 0$ . Conversely, for  $r > \frac{3q^2}{2m}$ , we have  $2mr - 3q^2 > 0$ , resulting in  $K < 0$ .

To obtain the curvature for the 4-dimensional case, we can derive the Riemann curvature tensor for the pseudo-Reissner-Nordström spacetime by applying a Wick rotation to the well-known Reissner-Nordström spacetime. This approach uses the established properties of the Reissner-Nordström solution, allowing us to modify the spacetime signature and adapt the curvature properties for the pseudo-Reissner-Nordström framework.

**6.1. Pseudo-Reissner-Nordström spacetime with two horizons.** The pseudo-Reissner-Nordström spacetime  $M = S^1 \times (0, \infty)$  with  $m > q$  and two horizons at  $r = r_{\pm}$  presents a particularly interesting configuration. These horizons divide  $M$  into three distinct regions:  $M_3 = \{(\nu, r) \in M \mid 0 < r < r_-\}$ ,  $M_2 = \{(\nu, r) \in M \mid r_- < r < r_+\}$ , and  $M_1 = \{(\nu, r) \in M \mid r_+ < r < \infty\}$ . In analogy with the pseudo-Schwarzschild spacetime, the coordinate vector field  $\partial_r$  is null, with  $-\partial_r$  designated as future-pointing (indicating that  $r$  decreases as one moves from past to future). The behavior of the vector field  $\partial_\nu$  varies across regions: it is spacelike in  $M_1$ , timelike in  $M_2$ , and again spacelike in  $M_3$ .

For radial null geodesics, we first set

$$ds^2 = -\left(\frac{2m}{r} - \frac{q^2}{r^2} - 1\right) d\nu^2 + 2drd\nu = 0,$$

from which we immediately see

$$\frac{d\nu}{dr} = \begin{cases} 2\left(\frac{2m}{r} - \frac{q^2}{r^2} - 1\right)^{-1} & (\text{outgoing}) \\ 0 & (\text{infalling}) \end{cases}.$$

In the next step we consider the outgoing radial null curves

$$d\nu = \frac{2}{-1 + \frac{2m}{r} - \frac{q^2}{r^2}} dr = \frac{2r^2}{R} dr = \frac{2r^2}{cr^2 + br + a} dr,$$

where  $R = 2mr - q^2 - r^2$ ,  $a = -q^2$ ,  $b = 2m$  and  $c = -1$ . This then takes the form of the integral  $\nu(r) = 2 \int \frac{r^2}{R} dr = 2(-r - m \ln R + (2m^2 - q^2) \int \frac{1}{R} dr)$ , where  $\Delta = 4ac - b^2 = 4(q^2 - m^2) < 0$ , and

$$\int \frac{1}{R} dr = \frac{1}{\sqrt{-\Delta}} \ln \frac{\sqrt{-\Delta} - (b + 2cr)}{(b + 2cr) + \sqrt{-\Delta}} = \frac{1}{\sqrt{-4(q^2 - m^2)}} \ln \frac{\sqrt{-4(q^2 - m^2)} - (2m - 2r)}{(2m - 2r) + \sqrt{-4(q^2 - m^2)}}.$$

From this we obtain  $\nu = \text{const}$  and

$$\nu(r) = 2 \left( -r - m \ln(2mr - q^2 - r^2) + (2m^2 - q^2) \left( \frac{1}{\sqrt{-4(q^2 - m^2)}} \ln \frac{\sqrt{-4(q^2 - m^2)} - (2m - 2r)}{(2m - 2r) + \sqrt{-4(q^2 - m^2)}} \right) \right).$$

Consequently, for large  $r$ , the slope of the light cones is  $\frac{d\nu}{dr} = \begin{cases} -2 \\ 0 \end{cases}$ , while as we approach  $r_+$ , the slope becomes  $\frac{d\nu}{dr} = \begin{cases} \rightarrow -\infty \\ 0 \end{cases}$ , and the light cones begin to open up once we cross the horizon (as illustrated in Figure 8). As we move closer to  $r_-$ , the light cones close up, giving  $\frac{d\nu}{dr} = \begin{cases} \rightarrow +\infty \\ 0 \end{cases}$ . We can traverse this horizon, and as the light cones tilt over, approaching the singularity at  $r = 0$ , the slope becomes  $\frac{d\nu}{dr} = \begin{cases} 0 \\ 0 \end{cases}$ .

In regions  $M_3$  and  $M_1$ , future-pointing paths move in the direction of decreasing  $r$ , while in region  $M_2$  this behavior conflicts with causality. The surfaces at  $r = r_{\pm}$  act as both chronology horizons and event horizons; crossing these horizons signifies a point of no return. For a particle initially starting its journey in region  $M_1$ , encountering the horizon at  $r = r_+$  is inevitable, while it is possible to accelerate away from the horizon at  $r = r_-$ .

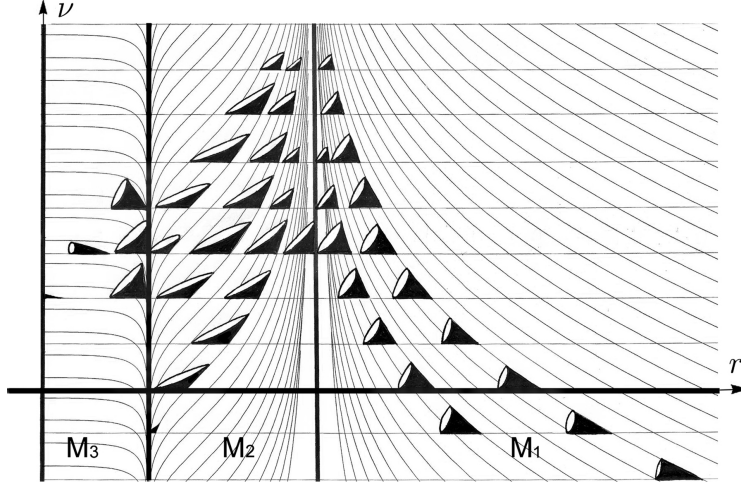


FIGURE 8. Spacetime diagram for the pseudo-Reissner-Nordström spacetime with two horizons.

6.1.1. Non-chronal region  $M_2$ . Although the closed timelike curves (CTCs) in this case primarily arise from the periodicity of the  $\nu$ -coordinate, the tilting of light cones also contributes to the formation of CTCs.

*Claim 6.1.* A causal curve  $\gamma : I \rightarrow M$  with velocity  $\gamma' = \gamma'_1 \partial_\nu + \gamma'_2 \partial_r$  is future-pointing if and only if  $\gamma'_1 \geq 0$ .

*Proof.* The inner product of two future-pointing causal vectors is non-positive. We already defined  $-\partial_r$  to be future-pointing, thus the claim follows directly from  $0 \geq g(\gamma', -\partial_r) = -\gamma'_1 \iff \gamma'_1 \geq 0$ .  $\square$

*Claim 6.2.* A curve  $\gamma : I \rightarrow M$  with velocity  $\gamma' = \gamma'_1 \partial_\nu + \gamma'_2 \partial_r$  is causal and future-pointing in  $M_2$  if and only if  $\frac{2 \cdot \gamma'_2}{(\frac{2m}{r} - \frac{q^2}{r^2} - 1)} \leq \gamma'_1$ . In  $M_1$  and  $M_3$ , it is causal and future-pointing if and only if  $\frac{2 \cdot \gamma'_2}{(\frac{2m}{r} - \frac{q^2}{r^2} - 1)} \geq \gamma'_1 \geq 0$ .

*Proof.* A future-pointing causal curve is a curve  $\gamma : I \rightarrow M$  satisfying that  $g(\gamma', \gamma') \leq 0$  and  $\gamma'_1 \geq 0$ . Hence,

$$\begin{aligned} 0 \geq g(\gamma', \gamma') &= g(\gamma'_1 \partial_\nu + \gamma'_2 \partial_r, \gamma'_1 \partial_\nu + \gamma'_2 \partial_r) = \gamma'_1 [2 \cdot \gamma'_2 - \gamma'_1 \cdot (\frac{2m}{r} - \frac{q^2}{r^2} - 1)] \\ \iff 2 \cdot \gamma'_2 - \gamma'_1 \cdot (\frac{2m}{r} - \frac{q^2}{r^2} - 1) &\leq 0 \iff 2 \cdot \gamma'_2 \leq \gamma'_1 \cdot (\frac{2m}{r} - \frac{q^2}{r^2} - 1). \end{aligned}$$

Now we have to discriminate between two cases:

- i)  $r_- < r < r_+ \implies (\frac{2m}{r} - \frac{q^2}{r^2} - 1) > 0: \frac{2 \cdot \gamma'_2}{(\frac{2m}{r} - \frac{q^2}{r^2} - 1)} \leq \gamma'_1$
- ii)  $0 < r < r_- \vee r_+ < r \implies (\frac{2m}{r} - \frac{q^2}{r^2} - 1) < 0: \frac{2 \cdot \gamma'_2}{(\frac{2m}{r} - \frac{q^2}{r^2} - 1)} \geq \gamma'_1,$

and this is precisely the assertion of the claim.  $\square$

The primary significance of this result lies in its identification of regions where closed timelike curves (CTCs) may occur, thereby justifying a focus on region  $M_2$ . The earlier identification of  $\nu = 0$  and  $\nu = \alpha$  leads directly to this outcome. On the hypersurfaces  $H_r$ , where  $r = \text{const}$ , the metric reduces to

$$g_{H_r} = -\left(\frac{2m}{r} - \frac{q^2}{r^2} - 1\right)d\nu^2,$$

which means that these surfaces are unconditionally spacelike when  $0 < r < r_- \vee r_+ < r$ . For a fixed value of  $r$ , the circle of constant radius  $\gamma_r = \{(\nu, r) \mid 0 \leq \nu \leq \alpha\}$  is timelike if  $r_- < r < r_+$ , spacelike if  $0 < r < r_- \vee r_+ < r$ , and null for  $r = r_{\pm}$ . This implies that a curve  $\gamma(s) = (s, r)$  with constant  $r \in (r_-, r_+)$  forms a closed timelike curve due to the periodicity of  $\nu$ , and when  $r = r_{\pm}$ , it forms a closed lightlike curve. Thus, we refer to  $r = r_{\pm}$  as the chronology horizon, and we designate the surfaces  $H_- := \{(\nu, r_-) \mid 0 \leq \nu \leq P\}$  and  $H_+ := \{(\nu, r_+) \mid 0 \leq \nu \leq P\}$ , with constant radii  $r_-$  and  $r_+$ , respectively, as the null hypersurfaces.

**Proposition 6.3.** *A closed timelike curve in  $M$  must lie entirely within region  $M_2$ .*

*Proof.* From what has already been proved, for a timelike future-pointing curve in  $M_1$  we have the requirement  $\frac{2}{\left(\frac{2m}{r} - \frac{q^2}{r^2} - 1\right)} < \frac{\gamma'_1}{\gamma'_2}$ . The procedure is to exclude that a timelike curve starts in region  $M_1$ , enters the region  $M_2$  and loops back to its initial point in  $M_1$ . Let us consider a timelike, future-pointing curve  $\gamma : [0, 1] \rightarrow M$  starting in  $M_1$ . The tangent vector to the curve is given by  $\gamma' = \gamma'_1 \partial_\nu + \gamma'_2 \partial_r$ , where  $\gamma'_1$  and  $\gamma'_2$  are the components of the tangent vector. Since the fundamental vector field  $\partial_r$  is null everywhere, and given that  $\gamma$  is future-pointing and timelike, we have  $\gamma'_1 > 0$  along the entire curve  $\gamma$ , and  $\gamma'_2 < 0$  for  $\gamma \subset M_1$ .

Assume  $\gamma(0) \in M_1$ , then  $\frac{2}{\underbrace{\left(\frac{2m}{r} - \frac{q^2}{r^2} - 1\right)}_{<0}} < \frac{\gamma'_1}{\gamma'_2}$  follows from the foregoing Lemma. As we approach the

Cauchy horizon  $H_+$  at  $r_+$ , we have  $\left(\frac{2m}{r} - \frac{q^2}{r^2} - 1\right) \rightarrow 0$ , and thus  $\frac{2}{\left(\frac{2m}{r} - \frac{q^2}{r^2} - 1\right)} \rightarrow -\infty$ . Consequently,  $-\infty < \frac{\gamma'_1}{\gamma'_2}$  as we approach  $H_+$ . The curve would remain in  $M_1$  and not enter region  $M_2$  only if  $\gamma'_2 = 0$ , meaning that it would be tangent to  $\partial_\nu$  and thus lightlike. However, since  $\gamma$  is timelike and  $\gamma'_2 \neq 0$ , it follows that the curve must enter the region  $M_2$ .

In region  $M_2$ , we have the requirement  $\gamma'_2 < \frac{\gamma_1 \cdot \left(\frac{2m}{r} - \frac{q^2}{r^2} - 1\right)}{2}$ . As  $r \rightarrow r_+$ , we observe that  $\frac{\gamma_1 \cdot \left(\frac{2m}{r} - \frac{q^2}{r^2} - 1\right)}{2} \rightarrow 0$ , and thus we can assert that  $\gamma'_2 < 0$  close to the horizon  $H_+$ . This shows that  $\gamma$  cannot cross the horizon  $H_+$  anymore and is therefore confined to region  $M_2$ . Consequently,  $\gamma$  cannot return to its initial position. In particular, it is evident that there are no closed timelike curves (CTCs) in region  $M_1$ , and similar considerations apply to region  $M_3$ .

It is immediately clear that a curve  $\gamma(s) = (s, r)$  with constant  $r \in (r_-, r_+)$  forms a closed timelike curve. According to Proposition 2.1, there are infinitely many CTCs in region  $M_2$ .  $\square$

The above arguments establish the following

**Corollary 6.4.** *There are closed timelike curves in  $M_2$ , and for every point  $p \in M_2$ , there exists a closed timelike curve passing through  $p$ .*

*Proof.* Under the conditions stated above, consider  $\gamma : [0, L] \rightarrow M, \gamma(s) = (ks, r), k \geq 0$ .  $\square$

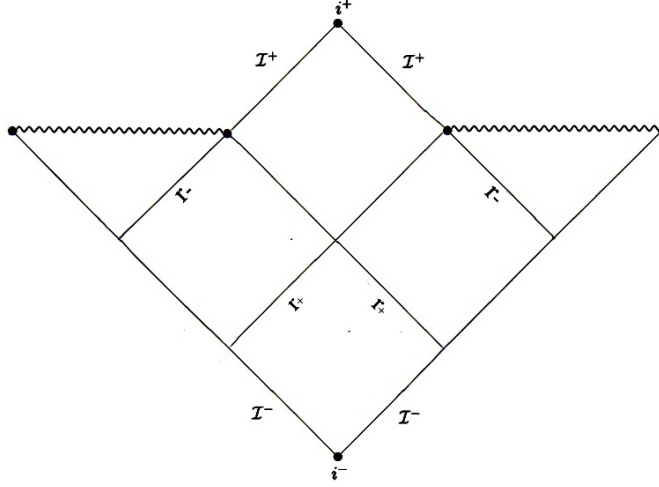


FIGURE 9. Conformal diagram for the pseudo-Reissner-Nordström spacetime with two horizons.

**6.2. Extremal pseudo-Reissner-Nordström spacetime.** The extremal 2-dimensional pseudo-Reissner-Nordström spacetime  $M$  with  $m = q$  has only one horizon at  $r = m$ , which separates  $M$  into two regions:  $M_3 = \{(\nu, r) \in M \mid 0 < r < m\}$  and  $M_2 = \{(\nu, r) \in M \mid m < r\}$ . As before, we time-orient  $M$  by requiring  $-\partial_r$  to be future pointing. The metric degenerates to

$$ds^2 = -\left(\frac{2m}{r} - \frac{m^2}{r^2} - 1\right)d\nu^2 + 2drd\nu = \left(\frac{m^2 - 2mr + r^2}{r^2}\right)d\nu^2 + 2drd\nu = \frac{(m-r)^2}{r^2}d\nu^2 + 2drd\nu.$$

The Gaussian curvature is

$$K = \frac{1}{2}S = -\frac{m(2r - 3m)}{r^4} = -R_{trtr},$$

where for  $r < \frac{3m}{2}$ , we have  $2mr - 3m^2 < 0$ , so the Gaussian curvature is  $\frac{2mr-3m^2}{r^4} > 0$ , and for  $r > \frac{3m}{2}$ , the curvature becomes negative.

By the same method as in Subsection 6.1, we calculate the radial null geodesics by setting

$$ds^2 = -\left(\frac{2m}{r} - \frac{m^2}{r^2} - 1\right)d\nu^2 + 2drd\nu = 0,$$

and we obtain

$$\frac{d\nu}{dr} = \begin{cases} 2\left(\frac{2m}{r} - \frac{m^2}{r^2} - 1\right)^{-1} & (\text{outgoing}) \\ 0 & (\text{infalling}) \end{cases}.$$

This term can be handled in much the same way as in Section 6.1, the only difference being that  $q = m$ . A quick verification shows that we obtain the integral  $\nu = \text{const}$ , and the expression for  $\nu(r)$  is

$$\nu(r) = 2 \left( -r + 2m \ln(r - m) - \frac{m^2}{m - r} \right).$$

Since  $g(\partial_r, \partial_r) = 0$  for all  $r \in (0, \infty)$ , we conclude that  $\partial_r$  is lightlike. Additionally, from  $g(\partial_u, \partial_u) = \frac{(m-r)^2}{r^2} > 0$  for all  $r \in (0, \infty)$ , we can deduce that  $\partial_u$  is spacelike at any point  $p \in M$ . See Figure 10.

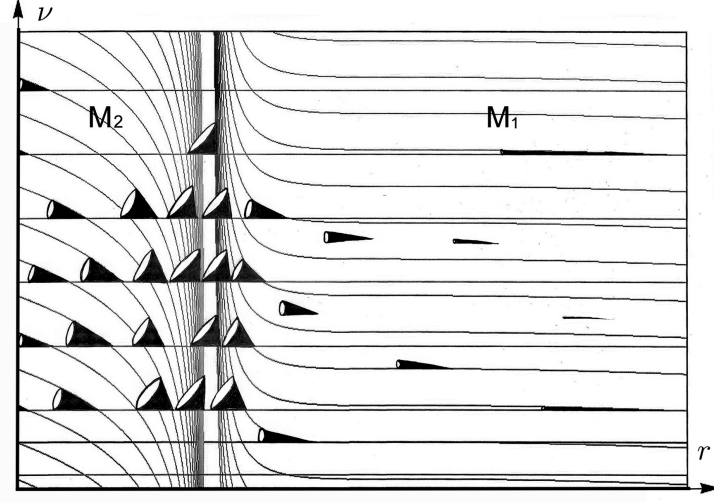


FIGURE 10. Light cone structure for the extremal pseudo-Reissner-Nordström spacetime.

**Proposition 6.5.** *A curve  $\gamma : I \rightarrow M$  with velocity  $\gamma' = \gamma'_1 \partial_\nu + \gamma'_2 \partial_r$  is causal and future-pointing in  $M$  if and only if  $2 \cdot \gamma'_2 \leq -\gamma'_1 \cdot \frac{(m-r)^2}{r^2}$ .*

*Proof.* A future-pointing causal curve is a curve  $\gamma : I \rightarrow M$ , satisfying that  $g(\gamma', \gamma') \leq 0$  and  $\gamma'_1 \geq 0$ . Hence,

$$\begin{aligned} 0 \geq g(\gamma', \gamma') &= g(\gamma'_1 \partial_\nu + \gamma'_2 \partial_r, \gamma'_1 \partial_\nu + \gamma'_2 \partial_r) = \gamma'_1 [2 \cdot \gamma'_2 + \gamma'_1 \cdot \frac{(m-r)^2}{r^2}] \\ \iff 2 \cdot \gamma'_2 + \gamma'_1 \cdot \frac{(m-r)^2}{r^2} &\leq 0 \iff 2 \cdot \gamma'_2 \leq \underbrace{-\gamma'_1 \cdot \frac{(m-r)^2}{r^2}}_{\leq 0}. \end{aligned}$$

□

We are now in the position to show

**Proposition 6.6.** *All future pointing causal curves in  $M_2$  converge towards the singularity  $r = 0$ .*

*Proof.* For a causal future-pointing curve  $\gamma : [0, 1] \rightarrow M_2 : s \mapsto \gamma(s)$  we have the requirement  $\gamma_1 \geq 0$ , and  $\gamma'_2 \leq \underbrace{-\gamma'_1 \cdot \frac{(m-r)^2}{r^2} \cdot \frac{1}{2}}_{\leq 0} \implies \gamma'_2 \leq 0$ . For  $\gamma'_2 = 0$  we have  $0 \leq \underbrace{-\gamma'_1 \cdot \frac{(m-r)^2}{r^2} \cdot \frac{1}{2}}_{\leq 0} \iff \gamma'_1 = 0 \vee \frac{(m-r)^2}{r^2} = 0$ .

Note that  $\gamma'_1 = 0$  implies, on the one hand, that  $\gamma' = \gamma'_1 \partial_\nu + \gamma'_2 \partial_r = 0$ , which means  $\gamma'$  is not future pointing.

On the other hand, the solution to  $\frac{(m-r)^2}{r^2} = 0$  gives  $r = m$ , which is the horizon and is not part of region  $M_2$ . Hence, we conclude that  $\frac{dr}{ds} = \gamma'_2 < 0$ , as claimed.  $\square$

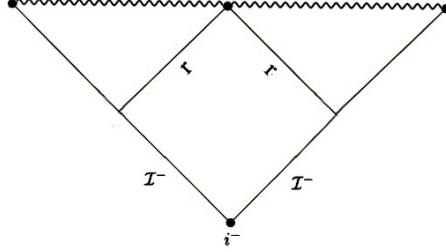


FIGURE 11. Conformal diagram for the extremal pseudo-Reissner-Nordström spacetime.

From these results, and given that  $r$  is strictly monotonic decreasing, we can conclude that for a future-pointing timelike curve—as defined above—it is impossible to form a closed curve. Therefore, the extremal pseudo-Reissner-Nordström spacetime does not contain closed timelike curves (CTCs). A closed lightlike curve exists only at  $r = m$ . Although the extremal pseudo-Reissner-Nordström spacetime does not permit closed timelike curves, a CTC almost emerges at  $r = m$ . If the light cones were to open up slightly more at that point, chronology would be violated.

**6.3. Pseudo-Reissner-Nordström timelike geodesics.** We first observe that the geodesics exhibit behavior similar to those in the pseudo-Schwarzschild or Misner space. This becomes evident when we write down the explicit timelike geodesic equation as a function of the radius by substituting  $g_{\nu\nu} = -\left(\frac{2m}{r} - \frac{q^2}{r^2} - 1\right)$  into Equation (3.7) in Section 3:

$$(6.4) \quad \nu(r) = \int \frac{\frac{-1}{\left(\frac{2m}{r} - \frac{q^2}{r^2} - 1\right)} \left( \xi - \omega \sqrt{\xi^2 - \left(\frac{2m}{r} - \frac{q^2}{r^2} - 1\right)} \right)}{\omega \sqrt{\xi^2 - \left(\frac{2m}{r} - \frac{q^2}{r^2} - 1\right)}} dr.$$

Such a timelike geodesic with  $\xi = 0$  encircles the horizon, while a geodesic with  $\xi > 0$  crosses the horizon. For the latter case we consider  $\xi^2 = \frac{2m}{r} - \frac{q^2}{r^2} - 1 \iff (\xi^2 + 1)r^2 - (2m)r + q^2 = 0$ .

By virtue of the discriminant

$$D = 4m^2 - 4q^2(\xi^2 + 1) \geq 0 \iff m^2 \geq q^2(\xi^2 + 1),$$

we obtain two potential turning points at

$$(6.5) \quad r_{turn1,2} = \frac{2m \pm \sqrt{4(m^2 - q^2(\xi^2 + 1))}}{2(\xi^2 + 1)} = \frac{m \pm \sqrt{m^2 - q^2(\xi^2 + 1)}}{(\xi^2 + 1)}.$$

As our focus in this work is to elaborate on and demonstrate the similarities between the three different spacetimes, we will disregard  $r_{turn2}$  and instead direct our attention to the region  $M_1 \cup M_2$ , specifically to the turning point contained within that region:

$$(6.6) \quad r_{turn1} = \frac{m + \sqrt{m^2 - q^2(\xi^2 + 1)}}{(\xi^2 + 1)}.$$

We observe an analogous situation to the pseudo-Schwarzschild case, where we obtain the corresponding turning point  $r_{turn} = \frac{2m}{(\xi^2 + 1)}$  when setting  $q = 0$ . The behavior of the null geodesics can be derived from the equation

$$\nu(r) = \int \frac{-1}{\left(\frac{2m}{r} - \frac{q^2}{r^2} - 1\right)} (\omega - 1) dr.$$

Analogous to the previously discussed cases, we have a set of null geodesics, specifically  $\nu(r) = \text{const}$ , that crosses the surfaces at  $r = r_{\pm}$ . These geodesics are complete and extend from  $r = 0$  to  $r = \infty$ . In contrast, another set of geodesics spirals around the horizons at  $r = r_{\pm}$ , and as a result, these geodesics are incomplete within this coordinate patch.

Due to the geodesic incompleteness, the embedded pseudo-Reissner-Nordström cylinder with  $\theta = \text{const}$  and  $\phi = \text{const}$ , restricted to  $M_1 \cup M_2$ , resembles the situation in the 2-dimensional Misner space and cylindrical pseudo-Schwarzschild spacetime.

## 7. CONCLUSION

We have investigated a family of causality-violating spacetimes—specifically, the pseudo-Schwarzschild, pseudo-Reissner-Nordström, and Misner spacetimes—that share fundamental causal structures, including the presence of chronology horizons, Cauchy horizons, radial geodesics, and acausal regions. All these spacetimes can be expressed in a warped product form, with metrics decomposing into the cylindrical metric  $g_Z$  and the hyperbolic metric  $g_{H^2}$ . This structure allows us to focus on their 2-dimensional cylindrical analogues. In Eddington–Finkelstein coordinates, these cylindrical versions can be brought to a canonical form  $ds^2 = g_{\nu\nu}d\nu^2 + 2g_{\nu r}d\nu dr$ , from which the radial geodesic equations (Section 3) can be systematically derived. Renaming the coordinates as  $\nu = \varphi$  and  $r = T$ , the connection to Misner spacetime becomes manifest.

In each case, the base manifold  $M_Z$  of the warped product structure is conformally related to a region of Minkowski spacetime and admits a Killing vector field whose orbits closely resemble those of the boost-generating vector field  $X = x \partial_t + t \partial_x$  in two-dimensional Minkowski space. This Killing vector field generates a one-parameter group  $G$  of isometries, some of whose orbits are timelike. A discrete subgroup  $G_0 \subset G$  acts properly and freely on  $M_Z$ , resulting in a Misner-like structure on the quotient  $M_Z/G_0$ , where the timelike orbits of  $G$  project to closed timelike curves.<sup>11</sup> From a mathematical standpoint, this conformal structure renders the similarities in causal properties relatively unsurprising, as they directly reflect known features of Misner spacetime. Nevertheless, from a physics perspective, the results are noteworthy. The spacetimes examined differ markedly in their physical interpretation and geometric origin—ranging from a flat vacuum

---

<sup>11</sup>As described in the classic book by Hawking and Ellis [11], Misner space is constructed by taking a quotient of half of Minkowski spacetime under a discrete subgroup of the one-parameter isometry group generated by the vector field  $X = x \partial_t + t \partial_x$ , which acts properly and freely in that region. A similar isometry group orbit structure appears in the  $(t, r)$ -planes of both the Schwarzschild and Reissner-Nordström spacetimes, allowing for analogous quotient constructions in these cases as well.

solution of the Einstein equations, to an asymptotically flat black hole solution of the vacuum Einstein equations, to a model that violates the weak energy condition and requires ‘exotic matter’ as its source—yet they exhibit analogous causal behavior. Understanding these similarities across physically distinct settings provides valuable insights into how causality can be broken or preserved under varying geometrical and physical conditions.

In the context of ongoing research on spacetimes with closed timelike curves [1, 4, 9, 19], our findings offer a unified framework to view several causality-violating spacetimes through a common geometric and causal lens. The work reveals the intricate relationships between these examples and motivates a broader investigation into the interplay between geometry, causality, and spacetime topology. For instance, it would be compelling to investigate whether other spacetime models, such as the pseudo-Kerr spacetime [3]—which is a rotating generalization of the pseudo-Schwarzschild metric and describes the spacetime around a rotating, uncharged, axially symmetric black hole —also belong to this family of causality-violating, Misner-type spacetimes.

Finally, this article proposes a conjecture concerning the isocausality of the spacetimes under consideration. A rigorous proof of the conjecture, as well as a deeper investigation into its physical implications, is left for future work. We view this article as a stepping stone toward a broader classification of causality-violating spacetimes. The ansatz presented here could be extended to more complex models, where tools such as isocausality may offer a systematic framework for organizing, comparing, and understanding their causal structures.

*Acknowledgement.* Parts of this work were completed during my time as a member of Richard Schoen’s research group at the University of California, Irvine. However, the research presented here originated from a project conducted under the supervision of Kip S. Thorne during 2016-2018. I am profoundly grateful to Kip S. Thorne for his invaluable advice, guidance, supportive remarks, and encouragement throughout the course of this work. I would also like to express my deep appreciation for his inspiring spirit of intellectual adventure in research and the insightful discussions, particularly on Misner space, which have been truly indispensable to this work. Furthermore, I am very grateful to the referees for their thorough and constructive feedback.

## REFERENCES

- [1] A. Awad and S. Eissa. Lorentzian Taub-NUT spacetimes: Misner string charges and the first law. *Phys. Rev. D*, 105 (2022), 124034.
- [2] S. Chandrasekhar. *The Mathematical Theory of Black Holes*. Clarendon Press, Oxford, England and Oxford University Press, New York (1983).
- [3] J. Dietz, A. Dirmeier and M. Scherfner. Geometric analysis of particular compactly constructed time machine spacetimes. *J. Geom. Phys.*, 62 (2012), 1273–1283.
- [4] R. Emparan and M. Tomašević. Quantum backreaction on chronology horizons. *J. High Energy. Phys.*, 2022, 182 (2022).
- [5] V. Frolov and I. Novikov. *Black Hole Physics: Basic Concepts and New Developments*. Springer Dordrecht (1998).
- [6] A. García-Parrado and J. M. M. Senovilla. Causal relationship: A new tool for the causal characterization of Lorentzian manifolds. *Class. Quantum Grav.* 20 (2003), 625–664.
- [7] A. García-Parrado and M. Sánchez. Further properties of causal relationship: Causal structure stability, new criteria for isocausality and counterexamples. *Class. Quantum Grav.* 22 (2005), 4589–4619.
- [8] M. Gaudin, V. Gorini, A. Kamenshchik, U. Moschella and V. Pasquier. Gravity of a static massless scalar field and a limiting Schwarzschild-like geometry. *Int. J. Mod. Phys. D* 15 (2006).
- [9] L. Gavassino. Life on a closed timelike curve. *Class. Quantum Grav.* 42 (2025), 015002.
- [10] R. Göhring. *Kosmologie der allgemeinen Relativitätstheorie*. Physikalischer Verein, Frankfurt am Main (2010).
- [11] S. W. Hawking and G. F. R. Ellis. *The Large Scale Structure of Space-Time*. Cambridge University Press, Cambridge (1973).

- [12] S. Kim and K. S. Thorne. Do vacuum fluctuations prevent the creation of closed timelike curves? *Phys. Rev. D*, 43 (1991), 3929.
- [13] D. A. Konkowski and L. C. Shepley. Stability of Two-Dimensional Quasisingular Space-Times. *Gen. Relativ. Gravit.* 14, No. 1 (1982).
- [14] C. W. Misner. Taub-NUT Space as a Counterexample to Almost Anything. *Relativity Theory and Astrophysics I: Relativity and Cosmology* (J. Ehlers Ed.), Lectures in Applied Mathematics 8 A.M.S. (1967).
- [15] C. W. Misner, K. S. Thorne and J. A. Wheeler. *Gravitation*. W. H. Freeman and Company, NY, San Francisco (1973).
- [16] A. Ori. Formation of closed timelike curves in a composite vacuum-dust asymptotically flat spacetime. *Phys. Rev. D*, 76 (2007), 044002.
- [17] D. Levanony and A. Ori. Extended time-travelling objects in Misner space. *Phys. Rev. D*, 83 (2011), 044043.
- [18] N. E. Rieger. Topologies of maximally extended non-Hausdorff Misner Space. [arXiv:gr-gc/2402.09312](https://arxiv.org/abs/2402.09312) (2024), digital preprint of the 2016 original version.
- [19] D. Roy, A. Dutta and S. Chakraborty. Geodesic Motion and Particle Confinements in Cylindrical Wormhole Spacetime: Exploring Closed Timelike Curves. *Int. J. Mod. Phys. A* (2025).
- [20] P. Sharan. *Spacetime, Geometry and Gravitation*. Springer, Birkhäuser Basel (2009).
- [21] K. S. Thorne. Closed Timelike Curves. *General Relativity and Gravitation; Proceedings of the 13th International Conference on General Relativity and Gravitation*, Institute of Physics Publishing, Bristol, England (1993), 295–315.
- [22] K. S. Thorne. Misner Space as a Prototype for Almost Any Pathology. *Directions in General Relativity* Eds. B. L. Hu et al., Cambridge University Press, Cambridge (1993), 333–346.